SYNTHESIS AND CHARACTERIZATION OF ULTRA-SMALL GADOLINIUM OXIDE NANOPARTICLES

A THESIS SUBMITTED TO
THE GRADUATE SCHOOL OF NATURAL AND APPLIED SCIENCES
OF
MIDDLE EAST TECHNICAL UNIVERSITY

BY
PAKİZAN TASMAN

IN PARTIAL FULFILLMENT OF THE REQUIREMENTS
FOR
THE DEGREE OF MASTER OF SCIENCE
IN
CHEMISTRY

SEPTEMBER 2017

Approval of the Thesis;

SYNTHESIS AND CHARACTERIZATION OF ULTRA-SMALL GADOLINIUM OXIDE NANOPARTICLES

submitted by **PAKİZAN TASMAN** in a partial fulfillment of the requirements for the degree of **Master of Science in Chemistry Department, Middle East Technical University** by,

Prof. Dr. Gülbin Dural Ünver
Dean, Graduate School of **Natural and Applied Sciences** _____

Prof. Dr. Cihangir Tanyeli
Head of Department, **Chemistry** _____

Prof. Dr. Mürvet Volkan
Supervisor, **Chemistry Department** _____

Examining Committee Members:

Prof. Dr. G. İnci Gökmen
Chemistry Department, METU _____

Prof. Dr. Mürvet Volkan
Chemistry Department, METU _____

Assoc. Prof. Dr. Murat Kaya
CEAC, Atılım University _____

Assist. Prof. Dr. Betül Sopacı
Chemistry Department, Ahi Evran University _____

Assist. Prof. Dr. Çiğdem Ay
Chemistry Department, Dumlupınar University _____

Date: 07.09.2017

I hereby declare that all information in this document has been obtained and presented in accordance with academic rules and ethical conduct. I also declare that, as required by these rules and conduct, I have fully cited and referenced all material and results that are not original to this work.

Name, Last name: Pakizan Tasman

Signature:

ABSTRACT

SYNTHESIS AND CHARACTERIZATION OF ULTRA-SMALL GADOLINIUM OXIDE NANOPARTICLES

Tasman, Pakizan

M.S., Department of Chemistry

Supervisor: Prof. Dr. Mürvet Volkan

September 2017, 54 pages

Ultra-small gadolinium oxide nanoparticles are used as contrast agents for molecular and cellular magnetic resonance imaging (MRI) procedure. They are also important for drug targeting magnetic separation and gene therapy applications due to their paramagnetic properties. Gadolinium oxide nanoparticles have been known to have the highest gadolinium density of all paramagnetic gadolinium contrast agents since they generate strong positive contrast enhancement. There are many techniques that have been introduced to synthesize gadolinium oxide nanoparticles. In this study, we optimized a simple polyol-free method for preparation of ultra-small nanosize (<4 nm) Gd_2O_3 nanoparticles. They are successfully synthesized in aqueous medium in an ultra-small nanosize 1.5-2.5 nm range which is the optimum size range needed for maximal contrast enhancement in MRI. After synthesizing gadolinium oxide nanoparticles, to analyze and characterize them, X-ray spectroscopy, scanning electron microscope (SEM), transmission electron microscope (TEM) and ultraviolet-visible

spectrophotometry (UV-VIS) were used. These nanoscale particles has been shown to have promising properties to function as a contrast agent for MRI imaging.

Keywords: magnetic resonance imaging MRI, contrast agent, synthesis, ultra-small gadolinium oxide nanoparticle.

ÖZ

ÇOK KÜÇÜK GADOLİNYUM OKSİT NANOPARTİKÜLLERİNİN SENTEZLENMESİ VE KARAKTERİZASYONU

Tasman, Pakizan

Yüksek Lisans, Kimya Bölümü

Tez Yöneticisi: Doç. Dr. Mürvet Volkan

Eylül 2017, 54 sayfa

Çok küçük gadolinyum oksit nanopartiküller, moleküler ve hücresel klinik öncesi manyetik rezonans görüntüleme prosedürlerinde kontrast madde olarak kullanılmaktadır. Ayrıca manyetik özellikleri sayesinde ilaç hedeflemede, manyetik ayırma ve gen terapi uygulamalarında da kullanılmaktadır. Bu nanopartiküller ürettikleri güçlü pozitif kontrast artış sayesinde, bütün paramanyetik gadolinyum kontrast maddeler arasında gadolinyum yoğunluğunun en yüksek olan nanopartiküller olarak bilinmektedir. Gadolinyum nanopartiküllerinin sentezlenmesi için birçok yöntem ve teknik açıklanmıştır. Bu çalışmada, çapı 4 nanometreden daha küçük gadolinyum oksit nanopartiküllerini basit ve poliolsüz bir yöntemle sentezlemeye çalışıldı. Su ortamında başarıyla sentezlenen bu nanopartiküller 1.5-2.5 nm aralığındadır ki, bu nano aralık manyetik rezonans görüntülemede en yüksek kontrastı verebilecek optimum boyut aralığıdır. Sentezlenen çok küçük gadolinyum oksit nanopartiküllerin analizi ve karakterizasyonu X-ray spectroskopi, taramalı elektron mikroskobu (SEM) ve geçirimli elektron mikroskobu (TEM),

Ultraviyole ve görünür ışık (UV-VIS) spektrometresi kullanılarak analiz edildi. Bu nano ölçekli parçacıklar, gelecekteki MRI işlemi için kontrast madde olarak gelecek vaat eden özelliklere sahiptir.

Anahtar kelimeler: Manyetik rezonans görüntüleme MRI, kontrast madde, sentez, çok küçük gadolinyum oksit nanopartikülleri.

To my dear family

ACKNOWLEDGEMENTS

I would like to thank to my supervisor Prof Dr. Mürvet Volkan for her endless guidance during my study. She has not only supported only my scientific side, also she develops my personality and perspective positively against then world.

I would like to express my special thanks to my dear assistant Yeliz Akpınar for her endless guidance and support during my whole study. She has always been helping me whenever I need. She has also been a great partner for me throughout the experiment, and helped me anytime I need. We really shared hard times while working in the lab until night, spent countless cheerful times together. I am really happy to have her in any part of my life.

I would like express my deepest gratitude to Assist. Prof. Dr. Betül Sopacı for valuable contribution to this thesis and for her patient guidance, and warm encouragement through my studies.

I would like to thank Assist. Prof. Dr. Çiğdem Ay for her guidance and help.

I would like to express my special thanks to Seçkin Öztürk for his endless support during our TEM, SEM analysis.

My special thanks to my labmates Zuhal Selvi Vanlı Güner. She was always with me even it gets harder, and helped me whenever I need. We have spent so many great times together.

I also want to thank my dear labmates; Merve Nur Güven, and Begüm Avcı for their valuable friendship, endless help and support. They always cheer me up when I get down morally. I am so happy to have them.

I would like to thank to Canan Höçük for being next to me anytime. She always encouraged me when I feel down, and helped me whenever I need. She became one of my best friends, and she always will.

I would like to thank Sezin Atıcı, Melis Çetmeli for their valuable friendship, endless help, and support. C-49 and C-50 become my second family.

I would like to thank my dearest friends Zehra Demir, Alev Bingöl, Fazıla Gelen. I also would like to thank Rabia Büşra Artan because she is my first best friend that this university gave me. They all deserve the sincere thanks for always being with me whenever I need them. I always found them next to me when I had a problem. They always encouraged me through the hardest times. I love them so much. I am so happy to have them in every part of my life.

Finally, my special thanks to my beloved ones my parents, Nezir Tasman and Feyziye Tasman. They always support me during my whole life. They are the ones who let me be who I am. I am so happy for being their daughter. And also special thanks to my dear siblings; Rezzan, İbrahim, Taha Salih for their endless, love patience, and moral support. They have never made me feel alone and desperate when I meet problem. They let me grow up in a peaceful life. I cannot express my deepest feelings in words towards my family for their sacrifice, motivation, and unconditional love. They always make me feel so lucky to have them. But especially I need to thank my dearest sister Rezzan for her endless support, patience, and help in any part of my life because I grow up with her. She always guided me whenever I need I am so happy to have her. I especially devote my thesis to her because I know that if I did not have her, I would not ever achieve to finish my master.

I also wish to thank all in Chemistry Department of METU.

This study was supported by a grant Project number: 115Z214 from The Scientific and Technological Research Council of Turkey Research Project Fund (TUBITAK).

TABLE OF CONTENTS

LIST OF TABLES

TABLES

LIST OF ABBREVIATIONS

MRI	Magnetic Resonance Imaging
SPIONs	Superparamagnetic Iron Oxide Nanoparticles
NSF	Nephrogenic systemic fibrosis
US-Gd_2O_3	Ultra-small gadolinium oxide nanoparticles
UV-VIS	Ultraviolet–visible spectroscopy
SEM	Scanning Electron Microscopy
CTEM	Conventional Transmission Electron Microscopy
XRD	X-ray Powder Diffraction
EDX	Energy-dispersive X-ray spectroscopy
TMAH	Tetramethylammonium Hydroxide

LIST OF FIGURES

FIGURES

CHAPTER 1

INTRODUCTION

1.1. An Introduction to Nanomaterials

Nanomaterials are chemical materials with a dimension in the nano scale, in a size range from 1 to 100 nm [1]. Nanoparticles have attracted an increasing attention since their properties are greatly changed at nano level owing to their large surface to volume ratio. The novel characteristic properties of nanoparticles can be presented as electronic, optical, magnetic, transport, photochemical, electrochemical, catalytic, and mechanism behavior when compared to their bulk counterparts [2-4]. Owing to these properties, nanoparticles gain new and unique capabilities to a variety of biomedical applications which is ranging from diagnosis of diseases to novel therapies [5].

1.2.Magnetic Resonance Imaging (MRI)

For living organisms, magnetic resonance imaging (MRI) is known to be one of the most powerful imaging techniques that is used to diagnose diseases, and it is also known as a very important noninvasive technique. MRI provides anatomically detailed images based on the soft tissue contrast and also provides functional information in a manner that is noninvasive and real time monitoring [6,7].

The working principle of the MRI process to create a clinical image can be given in three basic concepts. Firstly, signal is created from the MR properties,

secondly from these signals image is created, and then lastly tissue contrast is generated.

In signal creation process, the inherent susceptibility of hydrogen atoms to a magnetic field is applied as this property gives them the ability of aligning themselves along a dominant magnetic field. MRI does create the images of these hydrogen atoms in free water, proteins, lipids, etc. in the tissues under the investigation with applying a dominant external magnetic field. With application of this external magnetic field, protons (hydrogen atoms) rotate in a cone shaped fashion, which is termed as precession. Then a second, smaller, weaker magnetic field is generated by the precession of atoms. To perturb the magnetization of tissues, radiofrequency energy is applied in the presence of the strong external magnetic field. After application of radiofrequency pulse, the magnetization returns to its original unperturbed state. This recovery of magnetization occurs through different relaxation processes which are longitudinal magnetization, and transverse magnetization. While these relaxation processes are taking place, protons emit radio waves to be converted signals which are the second process of MR imaging. Finally, according to water content of tissues, contrast is generated to have 3D images of body and organs under investigation [8].

As mentioned above, through MRI, there are two different relaxation processes that are used for characterization of tissue and body organs: T1 which is known as longitudinal relaxation time, and T2 which is known as transverse relaxation time.

1.2.1. T1-Weighted Relaxation Process

Longitudinal relaxation, T1-weighted, is also referred to spin-lattice relaxation. When the spin system goes back to the equilibrium state in the z-direction following an excitation pulse, T1 relaxation process occurs. The protons emit their energy and relax to return to their original orientation. T1 is the time constant that describes the exponential growth process that is followed by the return of the net magnetization in the z-direction [8,9].

1.2.2. T2-Weighted Relaxation Process

Transverse relaxation, T2-weighted, is also known as spin-spin relaxation. T2 refers to the time is needed for 63% of the radiofrequency pulse generated by transverse magnetization to distribute. The main reason for this phenomenon is the loss of phase coherence between the processing protons in the transverse plane [8].

1.2.3. MRI Contrast Agents

MRI has further improved by the development of contrast agents. Contrast agents provide images of enlarging detectable organs and systems that are more specific and clear. They also provide a wide range of MRI applications for both diagnostic radiology and therapeutic medicine [7].

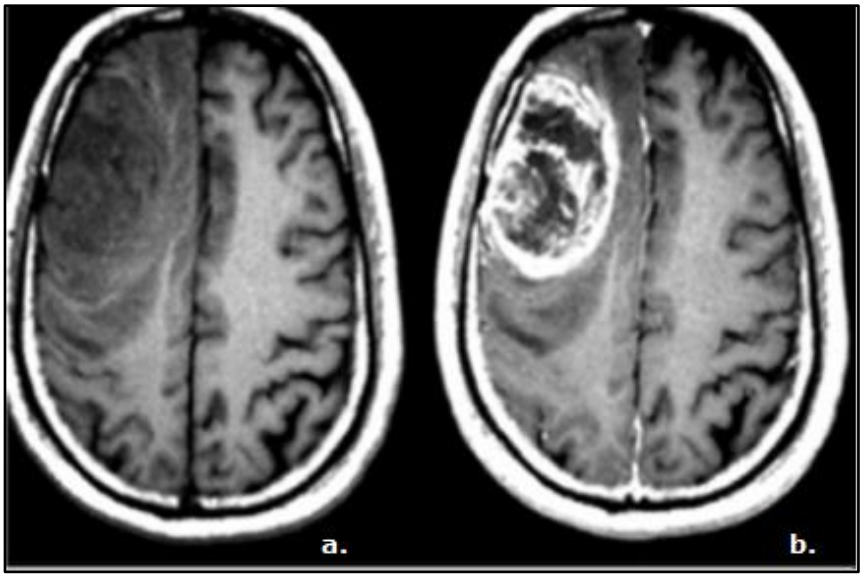

Figure 1 A brain MR image with Glioblastoma a. before the introduction of the contrast agent and b. after the introduction of the contrast agent [10].

Diseased tissues, such as tumors, cancer cells, have higher vascularity than healthy tissues which means that they have higher affinity for the introduced

contrast agent. Thus, when they are introduced to body, these contrast agents are preferentially up taken by such tissues, resulting in a higher and enhanced contrast in MRI images. Figure 1.a, and 1.b represent a brain image with glioblastoma which is a highly invasive, aggressive tumor formed in the brain, before and after the introduction of gadolinium-based contrast agent, respectively. As can be clearly seen in this figure, after the introduction of contrast agent, blood-brain barrier of tumor cells can be visualized more clearly. It can be said that as given in Figure 1, contrast agents are so important for such tumor imaging [10,11].

As mentioned before with details, MRI is an imaging procedure. Contrast agents are used to improve the quality of MRI images by controlling the longitudinal (the spin-lattice, $T1 = \frac{1}{r1}$) and the transverse (the spin-spin, $T2 = \frac{1}{r2}$) relaxation times of hydrogen (protons) of water available in the biological tissue or organs under investigation. Depending upon the chemical composition of contrast agent, T1 and T2 relaxation times of nuclei in the target tissue are reduced to different extents. According to their contrast effects in MRI, they deliver either positive contrast or negative contrast. Positive contrast is given by T1-weighted images while negative contrast is given by T2-weighted images. Until now, two main groups of contrast agents have been introduced for clinical purpose; superparamagnetic iron oxide nanoparticles (SPIONs) which are delivering negative contrast, and gadolinium-based paramagnetic agents which are delivering positive contrast [11-15].

SPIONs are negative contrast agents used in MRI owing to their superparamagnetism and their strong effects on T2 relaxation. Their ultra-small size leads to easy transportation of them across cell membranes. Labeling is possibly performed by the incubation of cells with contrast agent in vitro, so that they can be visualized in vivo utilizing MRI. SPIONs are not used only as contrast agent in MRI, but also used for drug/gene delivery, magnetic separation, magnetic hyperthermia for cancer treatment, and many other biomedical applications due to their magnetic properties and biocompatibility. They can be

synthesized in various shapes and sizes by using several techniques which enable them to be used in such extensive application areas [16][17]. However, these SPIONs suffer from some drawbacks. The signal strength in MRI is lowered by these particles; this causes low resolution, and delivering darker images. The clinical diagnosis in T2-weighted MRI can be misled by this resulting dark signals. Besides, SPIONs create signal voids in the MRI images that are so-called 'blooming artifacts' which make cell specification and characterization harder. In more detail, 'blooming artifacts' annihilate anatomical details around the cells and signal-based quantification studies are hindered or contrast alters. Then, MRI cannot differentiate the contrast between tissue and image artifacts due to the signals coming from bleeding, calcification, or metal deposits, and that is why the background image is distorted by the susceptibility artifacts. Another drawback of these negative contrast agents is that they have a large magnetic susceptibility. This feature of these nanoparticles affects an area that widens far beyond the volume of the labeled cells. Furthermore, while ultra-small SPIONs are specific to lymph nodes and bone narrow, SPIONs are specific to liver and spleen. That is why, it is said that these superparamagnetic iron oxide nanoparticles are not suitable for all organs while positive contrast agents are suitable for many organs to be used in MRI [7,9,13,14,18].

All these drawbacks of negative contrast agents (SPIONs) lead to further improvement of gadolinium-based positive contrast agents for MRI. Gadolinium-based positive contrast agents are becoming more popular due to their several advantages. They will be explained in detail in the next chapters.

1.3. Gadolinium

Gadolinium is an f-block element with electron configuration: [Xe] $4f^7 5d^1 6s^2$. In nature, gadolinium is mainly found in the minerals. It can be commercially separated by chemical treatments such as ion exchange and solvent extraction from the minerals monazite and bastnaesite. Also when it is used in alloys,

gadolinium has many useful properties such as being used for electronic components, for making magnets and as data storage disks. In this form, as an element, it does not have any biological role, and its toxicity is low. Its common oxidation state is 3 [19]. In its ionic form, Gd^{3+} has been known to be the best metal ion in the periodic table which can be used as positive contrast agent in MRI since its unpaired seven electrons in its 4f orbitals makes gadolinium to gain a large electronic magnetic moment. There is no other metal ion in the periodic table which possess unpaired electrons more than Gd^{3+} ion does [6,12].

In its element form Gd is not toxic, however, when it comes to its ionic form, free Gd^{3+} is highly toxic, and acts as an inorganic blocker in vivo since it tends to precipitate and be accumulated in liver, bones and lymph nodes which extend its half-life. Since its ionic radius which is 107.8 pm is nearly close to the ionic radius of Ca^{2+} which is 114 pm, and so causes the inhibition of physiological processes which depend on Ca^{2+} ions. Specifically, calcium-ion passage to muscle cells, the calcium flow in bone epiphyses and nerve tissue cells may be inhibited by free Gd^{3+} ion which causes the arrest of neuromuscular transmission. Also, free Gd^{3+} ion can replace some endogenous metals, more specifically zinc. This complication is known as transmetallation that can occur in the living organisms. To decrease toxic effect of Gd^{3+}ions in vivo, chelation has been applied to make them chemically inert. The chelation of Gd^{3+} ions increase the renal excretion rate nearly 550 fold when compared with values before chelation. That is why; highly stable gadolinium-based chelates have been developed to be used as positive contrast agents in MRI [20-22]. The gadolinium-based contrast agents will be explained in detail in the next section.

1.3.1. Gadolinium-Based Contrast Agents

Negative contrast agents, SPIONs, have still been used in many application areas including T2-weigthed MRI. Today, however, because of some drawbacks of SPIONs, explained in details in the previous chapter, the interest for negative

contrast agents has been decreased. That is why, gadolinium based contrast agents have gained more attention and importance. Now, scientists deal with increasing the MRI signal intensities by developing a new generation of gadolinium based contrast agents with further improved relaxation properties [14].

To get rid of high toxicity of free Gd^{3+} ions, gadolinium-based contrast agents are chelated. The first gadolinium based contrast agent was introduced by Runge in 1982 at the Radiologic Society of North America meeting in Chicago [23]. Then, in 1988, the first commercial MRI contrast agent that was proven to be used for clinical use is Magnevist (Berlex, Montville, NJ, USA) [24].

In Figure 2, the first contrast medium, Magnevist, and its organic chelate form are shown. It has been proven that is effective, and well tolerated by human body in more than 100 million investigations.

Figure 2 “Magnevist” is the first contrast medium that is introduced to worldwide usage in MRI [25].

After the introduction of Magnevist, other gadolinium based chelates have been developed, and approved to be used for clinical purposes. Some commercially available ones are given in Figure 3. There are also orally administered agents that have been approved. However, in clinical practice, they have not been

widely accepted. Scientists are still working for the improvement of contrast agents to create better resolution in MRI [26].

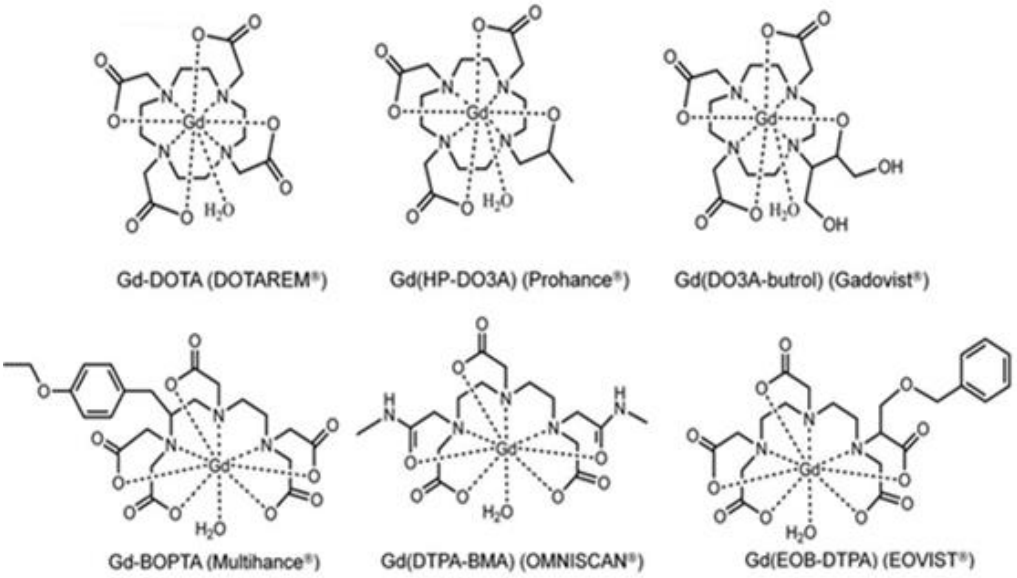

Figure 3 Some commercially used gadolinium chelates [27].

As mentioned before Gd^{3+} ions are highly toxic. That is why; to decrease heavy metal toxicity, gadolinium ion is chelated to form organic ligands, i.e. gadolinium chelates which are known as gadolinium-based contrast agents. However, although gadolinium chelates are widely used as positive contrast agents, their scope for prolonged imaging time is limited. This is because of their low molecular weight which leads to quick renal excretion. They are also limited for the possibilities of further chemical modifications [13,28]. Besides, the approved gadolinium chelates have historically been known to be safe. When it is used in patients with normal renal function at recommended dosing levels, it has been well tolerated and excreted from the body rapidly and completely in an intact state. However, in recent years, a rapidly growing body of data has been demonstrated that the accumulation of gadolinium is occurred in tissues, including brain, kidneys and bone of patients who have been exposed to gadolinium chelates during magnetic resonance imaging procedure, in spite of

normal renal function. It has been also recognized that the administration of gadolinium chelates has been associated with the development of nephrogenic systemic fibrosis in patients with severe renal insufficiency. Nephrogenic systemic fibrosis (NSF) is a disease that is potentially life-threatening, and debilitating. Indeed, the skin is predominantly affected but it can also affect other organs such as heart, the lungs, liver and muscles. It has been specifically reported that most cases of NFS have associated with the administration of gadolinium chelates which are gadopentetate dimeglumine (Magnevist), gadodiamide (Omniscan), and gadoversetamide (OptiMARK). With the growing data available, a safety announcement was published by the U.S. Food and Drug Administration (FDA) in July 2015 to investigate the risk of brain deposits associated with the repeated use of gadolinium chelates [12,29-33].

Such limitations of gadolinium chelates and the increasing demand for novel positive contrast agents has led to further development and improvement of ultra-small inorganic crystalline gadolinium based contrast agents nanoparticles (2–10 nm diameter) which are known to provide a rigid crystal environment. The release of gadolinium ions is expected to be effectively prevented by this new generation of nanoparticles. Gadolinium phosphate ($GdPO_4$), sodium gadolinium fluoride ($NaGdF_4$), gadolinium fluoride (GdF_3) and gadolinium oxide (Gd_2O_3) nanoparticles are such inorganic nanoparticles to be used as positive contrast agent in MRI [13,18,34].

The opportunity for extended imaging is provided by such nanoparticle contrast agents. Sodium gadolinium fluoride ($NaGdF_4$), gadolinium fluoride (GdF_3) is used to integrate optical and MR contrast effect into dual modality probes when doped with other lanthanides. Gadolinium oxide (Gd_2O_3) is known as promising T1 contrast agent with improved T1-weighted MR contrast enhancement. Besides, their surfaces are readily available for further chemical modifications [13, 32].

1.3.2. Ultra-Small Gd_2O_3 (US-Gd_2O_3) Nanoparticles

Gadolinium oxide nanoparticles have an important role in many biomedical applications such as multimodal imaging, drug delivery, and targeting the cancer cells. To be used for diagnosis and theranostics, they can be made multifunctional by biocompatible coatings, and further functionalization with suitable ligands [35, 36]. For example, Gd_2O_3 nanoparticles were functionalized by organic dye to be used as both magnetic resonance and fluorescence imaging [37].

Mean diameter of US-Gd_2O_3 nanoparticles is between 1-5 nm. They have been developed to be the best candidate for MRI as positive contrast agent for molecular and cellular preclinical MRI procedures [38]. Of all paramagnetic contrast agents, they have the highest gadolinium density. They also enhance T1-weighted MRI by generating strong positive contrast because of their seven unpaired 4f electrons of Gd. Being ultra-small nanoparticles makes them to provide the optimal surface to volume ratio which is necessary to obtain highest relaxivity in T1-weighted MRI [39].

US-Gd_2O_3 nanoparticles are prevailing in clinical usage since they are not only specific to some organs as superparamagnetic iron oxide nanoparticles. US-Gd_2O_3 nanoparticles are applicable for all organs such as liver, spleen, and lungs, etc. while SPIONS are more specifically used for liver [6, 40].

Being ultra-small (1-3 nm) is crucially important for gadolinium oxide nanoparticles since they can only provide higher spin-lattice relaxation rate (r1) in MRI if their mean diameter is less than 4 nm. Spin-lattice relaxation rate (r1) is directly related to the signal intensity of MR images. That is why, to have better MR images, and the highest longitudinal relaxation rate in T1-weighted MRI can only be provided by US-Gd_2O_3 nanoparticles with optimum nanosize range [12, 13]. It has been lately demonstrated that for maximum contrast enhancement in T1-weighted MRI, the optimum size of gadolinium oxide nanoparticles is 1-2.5 nm [6]. More specifically, it has been experimentally

demonstrated that this optimum size is nearly about 2.3nm [13]. Being ultra-small is also important for that the clearance of nanoparticles from the body. This process is done through the kidneys to avoid the accumulation of gadolinium oxide nanoparticles in the body. It has been known that the cutoff for renal excretion of nanoparticles needs to be below 10 nm. And generally, with decreasing particle size, renal excretion increases [41]. In addition to the advantage of renal clearance, working with ultra-small particles as MRI contrast enhancers have other advantages, such as prolonged examination time as a consequence of a prolonged circulation time. Small sized systems have an extended field of application because particle-cellular and particle-molecular interactions directly become feasible [14].

1.4. Encapsulation of US-Gd_2O_3 Nanoparticles within Ferritin Cage

US-Gd_2O_3 nanoparticles are used in multimodal imaging, drug delivery, and targeting the cancer cells [36, 42]. Their further stabilization and functionalization is done by surface coating with polyols and suitable ligands, by encapsulation with dendrimers to be used in biological applications as T1-weighted MRI contrast agents [18, 32, 43-46].

The synthesized US-Gd_2O_3 nanoparticles in the scope of this study will be used as positive contrast agents in T1-weigthed MRI. To be used for this purpose, they will be encapsulated within the apoferritin protein cage. As also shown in Figure 4, it is called apoferritin protein cage after dialysis of ferritin protein cage under N_2 against thioglycolic acid in a sodium acetate buffer at pH 4.5 [47]. Ferritin is an iron storage protein which shows a high level of structural similarity among a range of biological species such as animals, plants and microbial cells. That is why, in our studies, horse spleen ferritin will be used since its structural is similar to human ferritin. Ferritin is a spherical cage like protein composed of 24 subunits and inorganic iron core in a central cavity [48-52].

In Figure 4, schematic representation of dialysis of native ferritin to apoferritin is given. As mentioned above, apoferritin is obtained by dialysis of ferritin to be used as a core for synthesized nanoparticles.

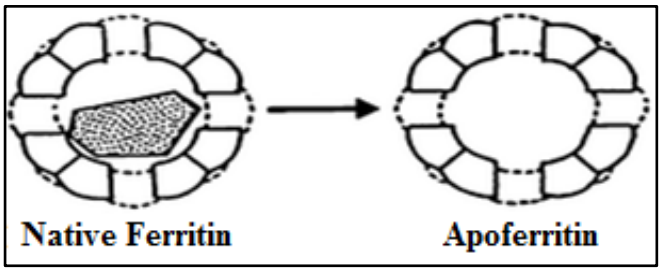

Figure 4 Schematic representation for dialysis of native ferritin [47]

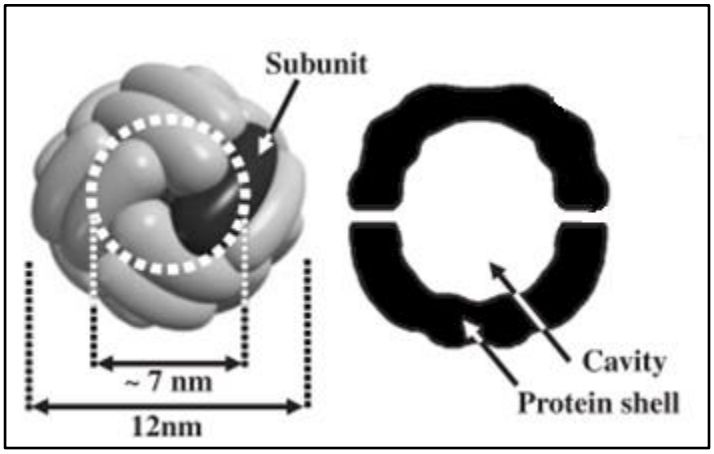

Figure 5 Schematic drawing of apoferritin [53].

As shown in Figure 5, apoferritin, consists of 24 subunits. One of them is shown with black color in Figure 5. The outer diameter of apoferritin is about 12 nm and its core size is about 7 nm. There are narrow channels connecting the inner cavity and outside, through which metal ions enter the inner cavity. The self-assembled protein cage has the ability to sequester and store iron as a hydrated iron oxide in the internal cavity [53-54].

1.5. Aim of This Study

The scope of this thesis was to synthesize ultra-small size, highly stable, monodisperse gadolinium oxide nanoparticles in aqueous medium. We aimed to optimize a simple polyol free method. Resulting Gd_2O_3 nanoparticles are also planned to be characterized by X-ray powder diffraction (XRD), spectroscopic (UV-Vissible) and by microscopic techniques (scanning electron microscopy-SEM and transmission electron microscopy- TEM). The synthesis of US-Gd_2O_3 nanoparticles is an initial step to have biocompatible and functionalized nanoparticles for MRI contrast enhancement. In the future, they will be encapsulated within the apoferritin protein cage.

CHAPTER 2

EXPERIMENTAL

2.1. Chemicals and Reagents

For all experimental procedure, 18.2 M Ω.cm ultra-pure deionized water from Elga, Purelab Option-Q Water Purification System was used. All chemicals were used as received.

2.1.1. Synthesis of US-Gd_2O_3 Nanoparticles via Polyol Method

To synthesize ultra-small Gd_2O_3 nanoparticles via polyol method, Gadolinium (III) chloride hexahydrate ($GdCl_3 \cdot 6H_2O$, 99.999% trace metals basis, SIGMA-ALDRICH), dried air, triethylene glycol (≥99%, SIGMA-ALDRICH) were used.

2.1.2. Synthesis of US-Gd_2O_3 Nanoparticles via Polyol-Free Method: Precipitation in Basic Medium

Gadolinium (III) nitrate hexahydrate ($Gd(NO_3)_3.6H_2O$, 99.9% trace metals basis, SIGMA-ALDRICH), tetramethylammonium hydroxide (1.0 M solution in water, A.C.S. reagent, SIGMA-ALDRICH), Ethyl acetate ($CH_3COOC_2H_5$, ACS, Reag., MERCK MILIPORE), Dimethyl sulfoxide pure (DMSO, $(CH_3)_3SO$, Atabay Kimya San. ve Tic. A.Ş.), Ammonium acetate ($CH_3CO_2NH_4$, ≥98%, SIGMA-ALDRICH), Ultra-pure deionized water, mili-Q water.

2.1.3. Synthesis of US-Gd_2O_3 Nanoparticles Polyol-Free Method with Citric Acid in Ethylene Glycol Medium

Gadolinium (III) chloride hexahydrate ($GdCl_3.6H_2O$, 99.999% trace metals basis, SIGMA-ALDRICH), Citric acid ($HOC(COOH)(CH_2COOH)_2$, SIGMA-ALDRICH), Sodium hydroxide (NaOH, 98-100.5%, pellets, SIGMA-ALDRICH), Ethylene glycol ($HOCH_2CH_2OH$, anhydrous, 99.8%, SIGMA-ALDRICH).

2.1.4. Synthesis of US-Gd_2O_3 Nanoparticles Polyol-Free Method with Citric Acid in Aqueous Medium

Gadolinium (III) chloride hexahydrate ($GdCl_3.6H_2O$, 99.999% trace metals basis, SIGMA-ALDRICH), Citric acid (CA, $HOC(COOH)(CH_2COOH)_2$, SIGMA-ALDRICH), Sodium hydroxide (NaOH, 98-100.5%, pellets, SIGMA-ALDRICH), Ethylene glycol ($HOCH_2CH_2OH$, anhydrous, 99.8%, SIGMA-ALDRICH), Ultra-pure deionized water, mili-Q water.

2.2. Instrumentation

2.2.1. X-ray Powder Diffraction (XRD)

XRD measurements of the synthesized US-Gd_2O_3 nanoparticles were carried out with a Rigaku Mini-Flex X-ray powder diffractometer using source of Cu Ka line radiation (λ=1.54056 Å). The range of 20-50 (2Θ) was scanned with a scan speed of 1.00. Samples were air dried powder for characterization.

2.2.2. Centrifugation

For washing process of US-Gd_2O_3 nanoparticles which were synthesized via polyol free method: precipitation in basic medium, a low-speed centrifuge

(NUVE, NF 200) was used for centrifugation of these nanoparticles. (Nüve, NF200). Samples were centrifuged at 4,060 rpm for 10 minutes.

2.2.3. Ultraviolet-Visible Spectrophotometry (UV-VIS)

Citric acid capped US-Gd_2O_3 nanoparticles were characterized by using UV/VIS Spectrometer (PG Instrument Ltd.) from 200 to 400 nm.

2.2.4. Scanning Electron Microscopy (SEM)

FEI QUANTA 400F Field Emission Scanning Electron Microscopy which is located at METU Central Laboratory was used to characterize the synthesized US-Gd_2O_3 nanoparticles.

2.2.5. Conventional Transmission Electron Microscopy (CTEM)

Conventional transmission electron microscopy (CTEM) measurements for the synthesized nanoparticles were performed on a FEI Tecnai G^2 Spirit BioTwin CTEM operated at 20 – 120 kV. It is located at METU Central Laboratory.

2.2.6. ImageJ Soft-Ware Program

ImageJ is an open source image processing program which is designed for scientific multidimensional images. This program was used to draw size distribution graphs of US-Gd_2O_3 nanoparticles. From SEM and CTEM images, 100 nanoparticles were randomly selected to measure their size by using ImageJ program. After measuring their mean diameter, their size distribution graphs were drawn [55].

2.3. Procedures

2.3.1. Synthesis of US-Gd_2O_3 Nanoparticles via Polyol Method

For the synthesis of US-Gd_2O_3 nanoparticles via polyol method, triethylene glycol was used as polyol solvent. One milimmole of $GdCl_3.6H_2O$ was mixed with 10 mL of triethylene glycol. This solution then was magnetically stirred at 100°C until $GdCl_3$ was completely dissolved the solvent. After dissolution, reaction temperature was increased to 250°-260°C and at that temperature for 24 hours was refluxed while air was passed through the solution. After 24 hours, the reaction solution was cooled to room temperature. Then, 1 L of de-ionized water added to the precipitate for washing, waited for 2 months for the reaction product to be settled down and the top solution was decanted. This washing procedure was repeated at least 4 times. However since the reaction product was not obtained as purely as desired to be used for characterization, any characterization results could not be obtained for this synthesis method [6].

2.3.2. Synthesis of US-Gd_2O_3 Nanoparticles via Polyol-Free Method: Precipitation in Basic Medium

To synthesize US-Gd_2O_3 nanoparticles via polyol-free method, gadolinium precursor was precipitated in basic medium. In this method, firstly, 6 mL of 0.067 M $Gd(NO_3)_3$ in DMSO was prepared. At room temperature, 2 mL of 0.55 M TMAH in ethanol was added to Gd^{3+} nitrate solution in a dropwise manner under constant stirring for 1 hour. While dropwise addition of TMAH, white precipitation of US-Gd_2O_3 nanoparticles was noticed. For washing process, ethyl acetate was added to the reaction solution to be washed by centrifugation at 4,060 rpm for 10 mins at least four times then diluted with deionized water. Then, to increase the water solubility, 0.056 g ammonium acetate was added to one whole batch. Then powder samples were air dried to be characterized [14].

In Figure 6, synthesized US-Gd_2O_3 nanoparticles were observed as white precipitate while dropwise addition of TMAH.

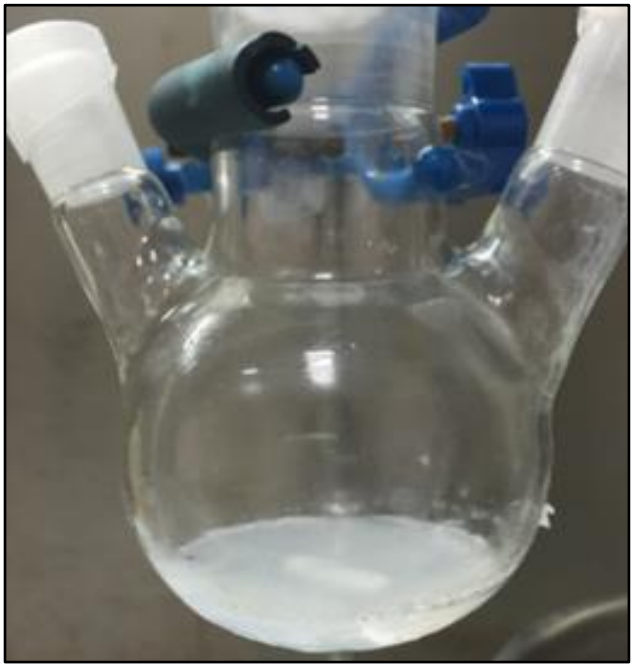

Figure 6 Synthesized US-Gd_2O_3 nanoparticles were observed as white precipitate while dropwise addition of TMAH.

2.3.3. Synthesis of US-Gd_2O_3 Nanoparticles with Polyol-Free Method with Citric Acid in Ethylene Glycol Medium

For synthesis of US-Gd_2O_3 nanoparticles via polyol-free method, citric acid was used as capping agent in ethylene glycol medium. 0.050 M of $GdCl_3.6H_2O$ was prepared in ethylene glycol, which corresponds to 0.3717 g of $GdCl_3.6H_2O$ in 20 mL of ethylene glycol. $GdCl_3.6H_2O$ was thoroughly dissolved using an ultrasonic bath for approximately 10 min. Then, 0.1921 g of citric acid (corresponds to 1.0 M of citric acid in 20 mL of ethylene glycol solution) was added to the solution to be dissolved in the ultrasonic bath for approximately 5 min. Finally, 1 mL of 6 M NaOH was added in a dropwise manner under

sonication. Stoichiometrically, 3 M NaOH was expected to be enough for a $GdCl_3.6H_2O$ concentration of up to 0.05 M, but since it has been known that free Gd^{3+} ions are toxic for the biological tissues, excess amount of NaOH was added to get rid of these free Gd^{3+} ions. After completion of addition of NaOH, the overall solution was kept in the ultrasonic bath for another 45 min. Steric stabilization of US-Gd_2O_3 nanoparticles is provided by citric acid with three carboxyl groups, also the concentration of citric acid can be used to control the size of nanoparticles. Moreover, it can be said that synthesized nanoparticles via this method are stable for weeks and the reproducibility of the method is high. The temperature for this synthesis method was 60°C [40].

In Figure 7, US-Gd_2O_3 nanoparticles which were synthesized in ethylene glycol medium is given.

Figure 7 US-Gd_2O_3 nanoparticles which were synthesized by using citric acid in ethylene glycol medium.

2.3.4. Synthesis of US-Gd_2O_3 Nanoparticles Polyol-Free Method with Citric Acid in Aqueous Medium

For the synthesis of US-Gd_2O_3 nanoparticles, a slightly modified synthetic route, which was reported earlier [40], was applied. 0.6 M citric acid was prepared by addition of 1.153 g of citric acid in 10 mL ultra-pure deionized water to be dissolved in the ultrasonic bath for 5 min. Then 0.1359 g of $GdCl_3.6H_2O$ was added to citric acid containing solution to be dissolved under continuous sonication for approximately 10 min. Then, 0.5 mL of 6 M NaOH was added to reaction solution in a drop-by-drop manner. For 1 hour, the overall solution was kept in the ultrasonic bath. By changing concentration of citric acid, particle size can be controlled [13].

In Figure 8, US- Gd_2O_3 nanoparticles that were synthesized by using citric acid in aqueous medium is given.

Figure 8 The synthesized US-Gd_2O_3 nanoparticles by using citric acid in aqueous medium.

CHAPTER 3

RESULTS AND DISCUSSION

In the scope of this thesis, US-Gd_2O_3 (1-3 nm) nanoparticles was synthesized by using both polyol, and polyol-free methods to compare each methods and to discuss advantages and disadvantages of the methods. After synthesizing US-Gd_2O_3 nanoparticles by using different methods, they are characterized by spectroscopic and microscopic techniques to define structure, morphology and size of these nanoparticles.

3.1. Preparation of US-Gd_2O_3 Nanoparticles via Polyol Method

To synthesize US-Gd_2O_3 nanoparticles via polyol method was the starting point to synthesize them in ultra-small nano range since it is known that polyols are used as stabilizer to control particle size growth. Polyols are alcohols that have high boiling point. They also prevent agglomeration [56]. This method was applied for the synthesis of gadolinium oxide nanoparticles; however characterization of the nanoparticles synthesized by this method could not be achieved. The main reason is that each washing process takes about two months. In order to get rid of polyol impurities, the synthesized nanoparticles were needed to be washed at least five or more times. Although the synthesized nanoparticles were washed with de-ionized water, the reaction product was not obtained as purely as desired to be used for characterization.

3.2. Preparation of US-Gd_2O_3 Nanoparticles via Polyol-Free Method: Precipitation in Basic Medium

To find out the optimum conditions to have ultra-small, monodisperse gadolinium oxide nanoparticles, different parameters were changed. The reaction temperature was changed between 8°C and 40°C while it was given in the article as room temperature. The stoichiometric ratio between precursor and base in literature was 1:1 [14]. This ratio was changed as another parameter. The base amount was decreased to half. In the literature, the reaction product was washed with ethyl acetate, but ethanol was used in our study as a washing solvent to find out if we can have more dispersed nanoparticles for characterization studies [14].

As can be seen from Table 3.1, nanoparticles were synthesized by changing different parameters to achieve the optimum conditions. Optimum condition is the condition that is needed to synthesize the highly dispersed ultra-small nanoparticles.

Table 1 Different parameters tried to find the optimum conditions for polyol-free method: precipitation in basic medium.

	Temperature (°C)	Precursor:Base Ratio	Washing Solvent
Sample 1	20 °C	1:1	EtOAc
Sample 2	10°C	1:1	EtOAc
Sample 3	25°C	1:1	EtOAc
Sample 4	25°C	2:1	EtOAc
Sample 5	40°C	2:1	EtOAc
Sample 6	30°C	2:1	EtOAc
Sample 7*	30°C	1:1	EtOAc
Sample 8	8°C	1:1	EtOAc
Sample 9	30°C	1:1	EtOAc/Ethanol
Sample 10	30°C	1:1	Ethanol/EtOAc
Sample 11	30°C	1:1	Ethanol

* Sample 7: Optimum condition that was achieved through these parameters.

To decide optimum conditions for this synthesis method, X-ray Powder Diffraction (XRD) analysis was used. When a broad peak centered at 2 Theta (2Θ) ≈29° which is the characteristic peak for the Gd_2O_3 was observed in XRD pattern of synthesized nanoparticles, then scanning electron microscopy (SEM) and conventional transmission electron microscopy (CTEM) were used as further characterization [14]. It was found that the optimum condition for the synthesis of US-Gd_2O_3 nanoparticles is 30°C, precursor to base ratio as 1:1, and

ethyl acetate as washing solvent. All characterization results were obtained from Sample 7 that was synthesized according to given parameters.

While preparing sample for characterization through XRD, the reaction product was washed by centrifugation at 4,060 rpm for 10 mins with ethyl acetate four times, and then air dried. Figure 9 represents the XRD pattern of Gd_2O_3 nanoparticles synthesized by precipitation in basic medium, a polyol free method. The gadolinium oxide nanopowder displays one broad peak centered at 2 Theta (2Θ) ≈29° which is the characteristic peak for the Gd_2O_3 [14]. As can be seen in Figure 9, the extensive broad peak around 29° provides us that our synthesized particle has small nanoparticle size in the range of nanometer.

Figure 9 shows XRD pattern of Gd_2O_3 nanoparticles synthesized via polyol free method: Precipitation in basic medium is given.

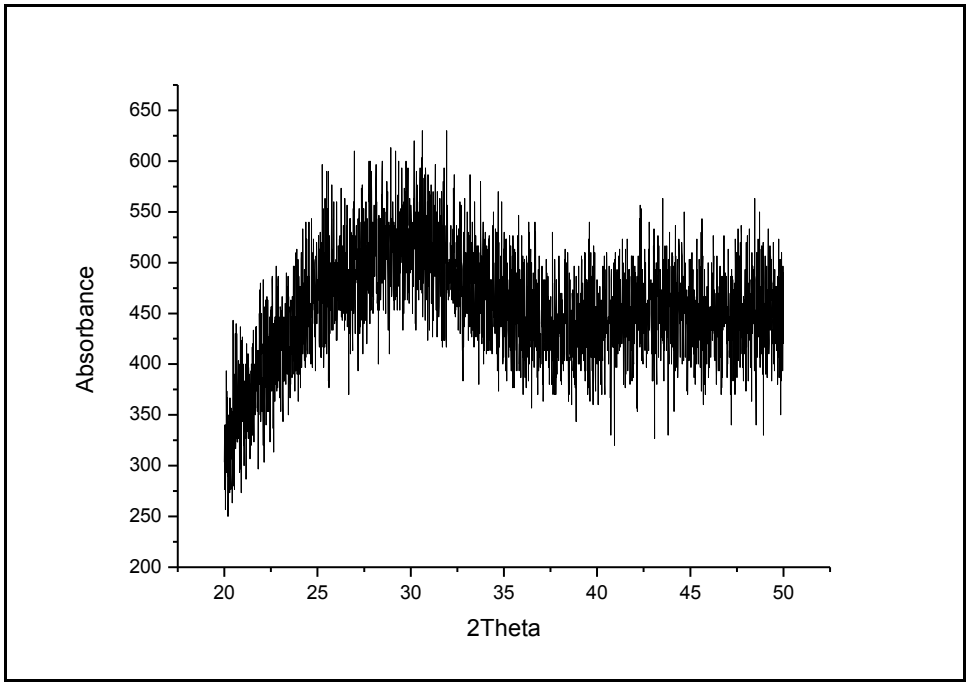

Figure 9 XRD pattern of Gd_2O_3 nanoparticles synthesized via polyol free method: Precipitation in basic medium.

To characterize the synthesized gadolinium oxide nanoparticles, scanning electron microscopy (SEM) was used as another characterization technique.

SEM samples were prepared on a silicon wafer. In Figure 10, SEM image of synthesized nanoparticles is shown. The size distribution graph was drawn by using ImageJ program with randomly selected 100 particles from SEM image that was taken. From SEM image and the size distribution graph of randomly selected 100 nanoparticles, they have size distribution between 20-50 nm. According to the size distribution graph, mean diameter of more than seventy percent of these nanoparticles is found between 20-50 nm.

SEM image and the size distribution of synthesized US-Gd_2O_3 nanoparticles by using precipitation in basic medium method, a polyol free method, can be seen in Figure 10 and Figure 11 respectively.

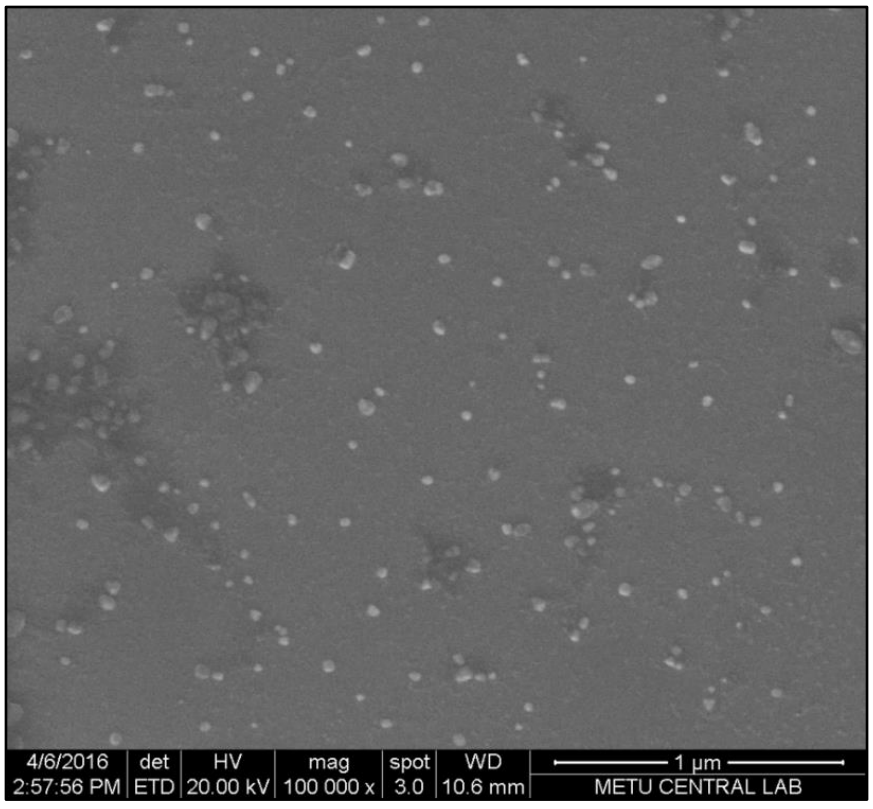

Figure 10 SEM pattern of Gd_2O_3 nanoparticles synthesized via polyol free method: Precipitation in basic medium.

Figure 11 represents the size distribution graph of Gd_2O_3 nanoparticles synthesized via polyol free method: Precipitation in basic medium is given.

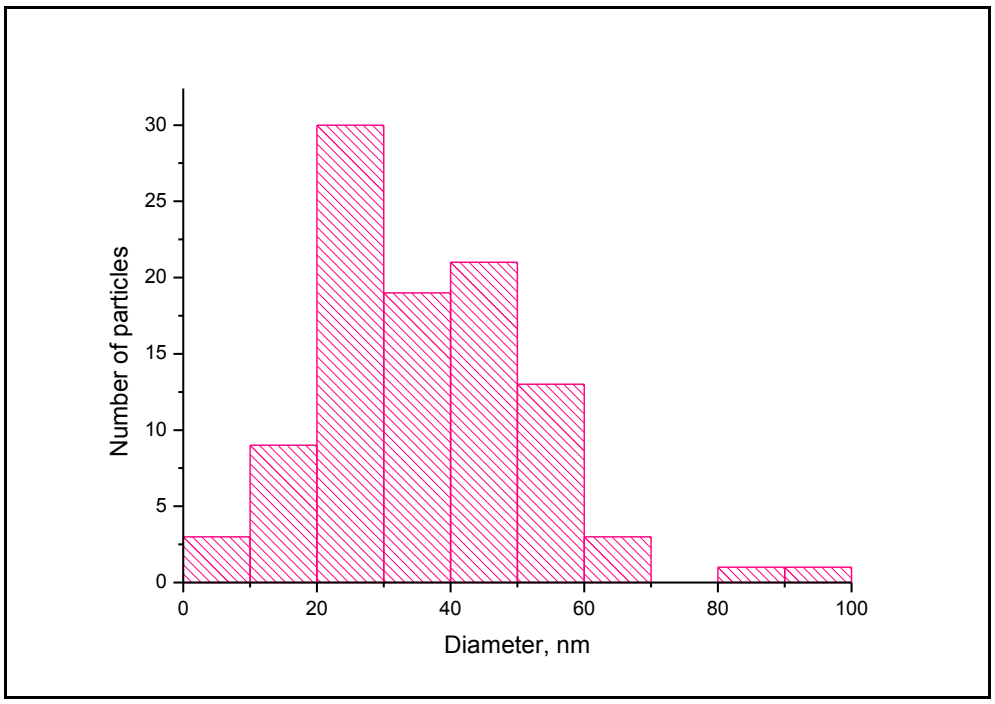

Figure 11 Size distribution graph of Gd_2O_3 nanoparticles synthesized via polyol free method: Precipitation in basic medium.

Energy-dispersive X-ray spectroscopy (EDX) pattern gives elemental analysis information about synthesized particles. EDX pattern of gadolinium oxide nanoparticles is taken during scanning electron microscopy analysis. To interpret the peaks observed in EDX pattern, it can be said that Ca and C may come from insufficient washing process, and ionized water. The strongest Si peak comes from Si wafer plate that is used for SEM analysis. As we expected, Gd and O peaks are available in EDX pattern.

In Figure 12, EDX pattern of synthesized Gd_2O_3 nanoparticles by using precipitation in basic medium method, a polyol free method, can be seen.

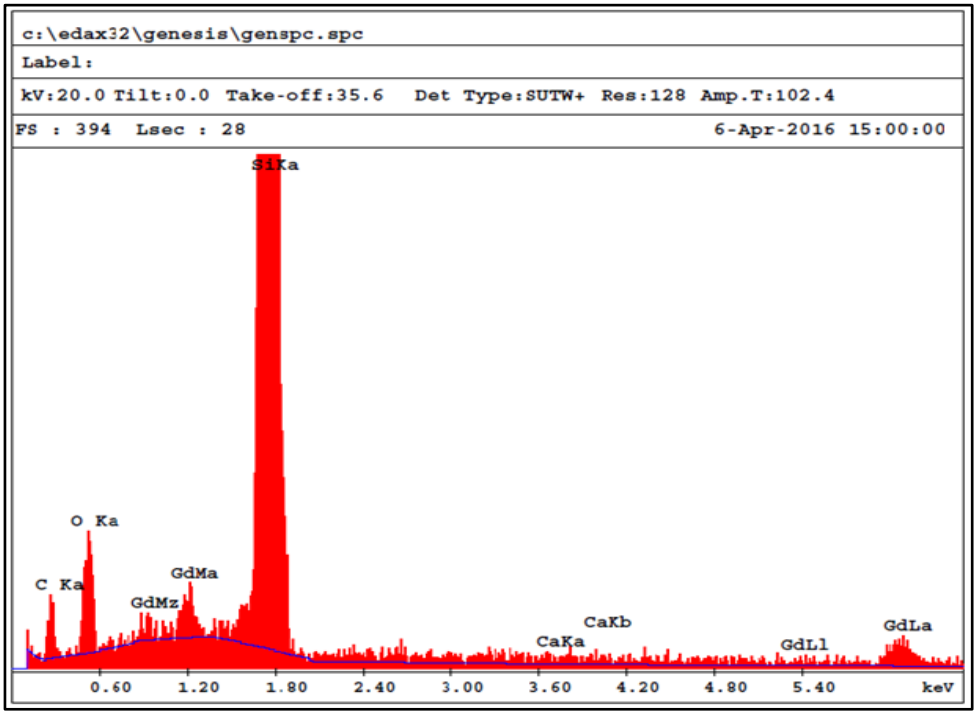

Figure 12 EDX pattern of Gd_2O_3 nanoparticles synthesized via polyol free method: Precipitation in basic medium.

Another characterization technique is conventional transmission electron microscopy (CTEM). Sample preparation for CTEM imaging was done by diluting Gd_2O_3 nanoparticles in water. Then 5 µL of diluted solution was dropped on amorphous carbon coated 200 mesh grid for characterization. In Figure 13, CTEM image of synthesized Gd_2O_3 nanoparticles is shown. The sample was washed with ethyl acetate by using centrifugation many times. The agglomeration has been observed according to CTEM image. SEM and CTEM images were not taken at the same time. CTEM images were taken after nearly one month later than SEM analysis. That is why; this agglomeration may cause from that sample was waited nearly about a month. Size, shape, and size

distribution of the nanoparticles cannot be estimated by this CTEM image because of agglomeration.

In Figure 13, CTEM image of the synthesized US-Gd_2O_3 nanoparticles via polyol-free method: Precipitation in basic medium is given.

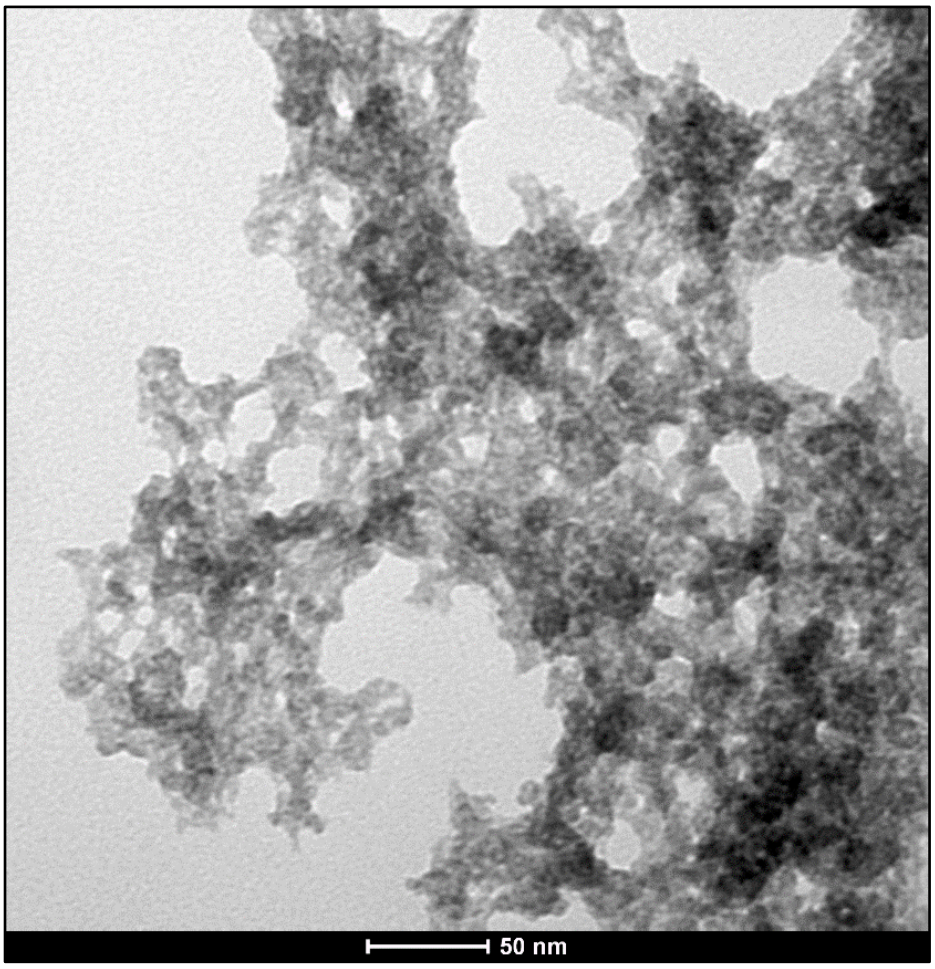

Figure 13 CTEM image of the synthesized Gd_2O_3 nanoparticles via polyol-free method: Precipitation in basic medium.

3.3. Preparation of US-Gd_2O_3 Nanoparticles with Polyol-Free Method with Citric Acid in Ethylene Glycol Medium

For the synthesis of US-Gd_2O_3 nanoparticles, citric acid was used as capping agent in ethylene glycol medium. According to given procedure in the article, it has been emphasized that size of nanoparticle decreases with increasing molarity of citric acid to be used [40]. Therefore, to have smaller gadolinium oxide nanoparticles, the higher molarity of citric acid, 1.0 M, was used.

For characterization of nanoparticles, UV-VIS spectrometry was firstly utilized. The peaks observed in the UV-VIS spectrum are interpreted according to transition states of 4f orbitals of gadolinium. The most intense peak appears at around 228 nm and can be assigned to $^8S_{7/2}$ to $^6D_{9/2}$ transition. The absorption peak at 274 nm is characteristic for all Gd_2O_3 particles and may be attributed to $^8S_{7/2}$ to $^6I_{7/2}$ transition [40]. These peaks prove us that synthesized nanoparticles are gadolinium oxide nanoparticles.

In Figure 14, UV-VIS spectrum of the synthesized US-Gd_2O_3 nanoparticles via polyol free method with using citric acid in ethylene glycol medium is given.

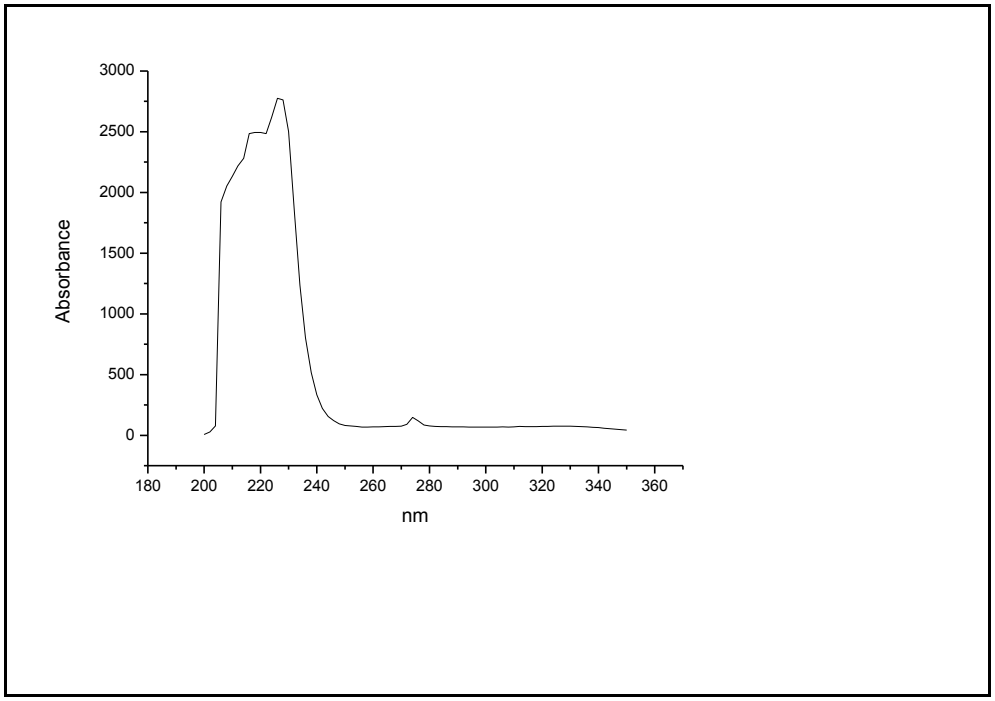

Figure 14 UV-VIS spectrum of the synthesized US-Gd_2O_3 nanoparticles via polyol free method with using citric acid in ethylene glycol medium.

For further characterization, CTEM image of these nanoparticles was taken. Sample preparation for CTEM imaging was done by letting 1–2 drops of Gd_2O_3 in ethylene glycol medium to dry on an amorphous carbon coated 200 mesh grid. CTEM image of Gd_2O_3 nanoparticles as synthesized using citric acid in ethylene glycol medium through polyol free method, and their size distribution graph can be seen in Figure 15, and Figure 16, respectively. From CTEM image, it can be said that synthesized nanoparticles are highly monodispersed in ethylene glycol medium. The size distribution graph also supports their monodispersity. The size distribution graph was drawn by using ImageJ program with randomly selected 100 particles from CTEM image. According to this graph, more than fifty percent of synthesized gadolinium oxide nanoparticles have narrow size distribution between 2-4 nm which means they are ultra-small nanoparticles.

In Figure 15, CTEM image of synthesized US-Gd_2O_3 nanoparticles via polyol free method by using citric acid in ethylene glycol medium is given.

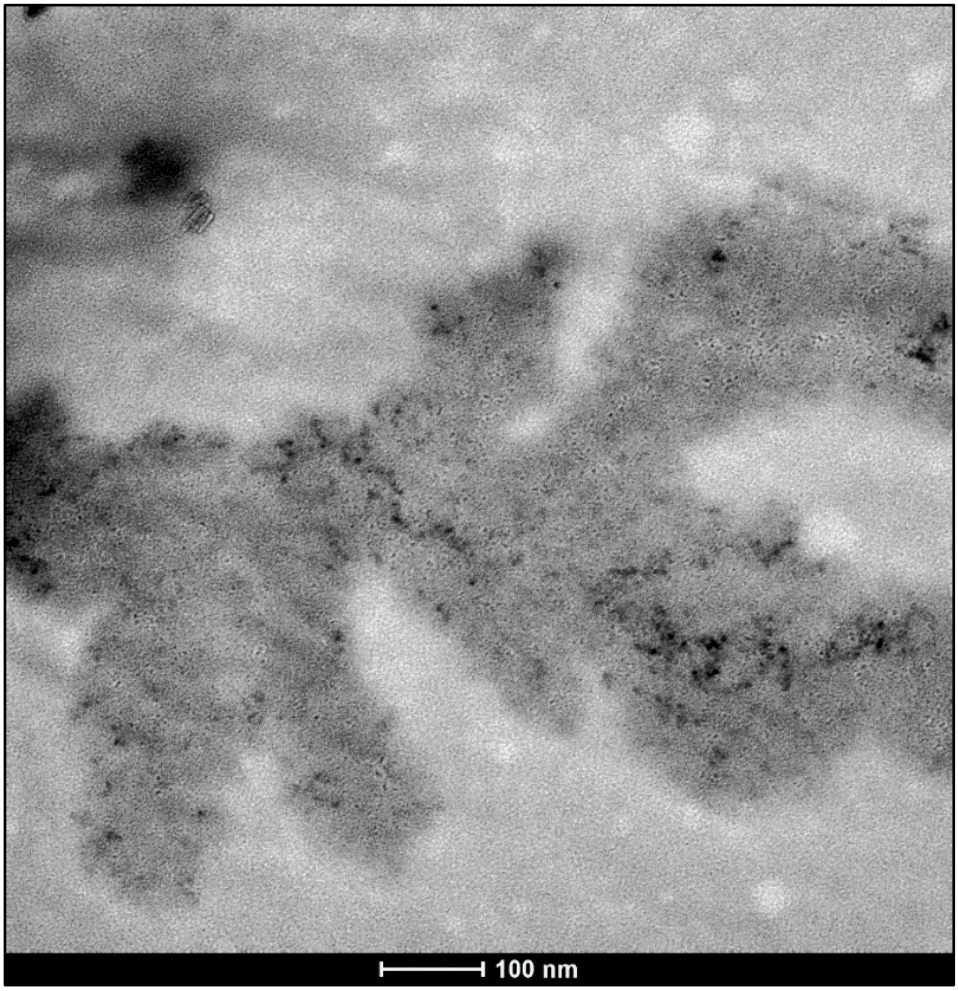

Figure 15 CTEM image of synthesized US-Gd_2O_3 nanoparticles via polyol free method by using citric acid in ethylene glycol medium.

In Figure 16, the size distribution graph of synthesized US-Gd_2O_3 nanoparticles via polyol free method by using citric acid in ethylene glycol medium is given.

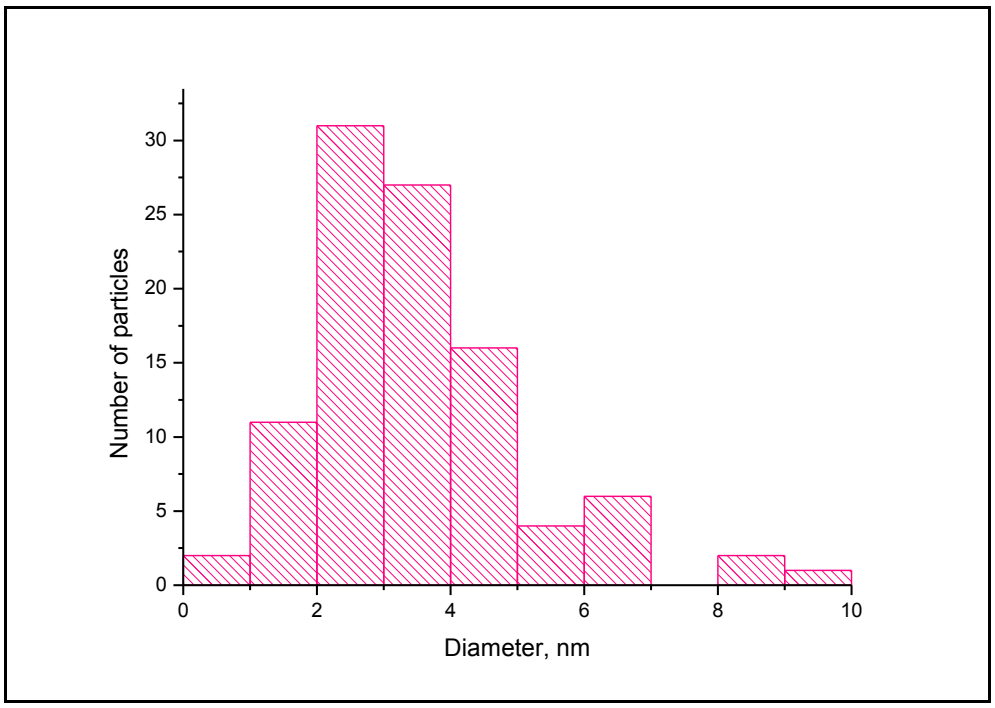

Figure 16 Size distribution graph of synthesized US-Gd_2O_3 nanoparticles via polyol free method by using citric acid in ethylene glycol medium.

3.4. Preparation of US-Gd_2O_3 Nanoparticles Polyol-Free Method with Citric Acid in Aqueous Medium

To synthesize US-Gd_2O_3 nanoparticles in aqueous medium, the previous method is further modified [13]. In the previous method, ethylene glycol was used as medium. However, since these nanoparticles will be used in bioactivity analysis, it has been tried to synthesize nanoparticles in aqueous medium. That is why, in this modified method, ultra-pure deionized water was used as medium. The size of synthesized nanoparticles is dependent on molarity of citric acid. After trying to synthesize nanoparticles with different molarities of citric acid, the optimum molarity, which was decided by utilizing UV-VIS spectrometry, was found as 0.6 M citric acid. Sample was firstly characterized by utilizing UV-VIS spectroscopy.

As in the same for the first synthesis method of gadolinium oxide nanoparticles in ethylene glycol medium, the peaks observed in the UV-VIS spectrum are interpreted according to transition states of 4f orbitals of gadolinium. As can clearly be seen from Figure 17, UV-VIS spectrum, the most intense peak appears at around 228 nm and can be assigned to $^8S_{7/2}$ to $^6D_{9/2}$ transition. The absorption peak at 274 nm is characteristic for all Gd_2O_3 particles and may be attributed to $^8S_{7/2}$ to $^6I_{7/2}$ transition [40]. We can say that these peaks prove us that nanoparticles observed in CTEM images are gadolinium oxide nanoparticles.

In Figure 17, UV-VIS spectrum of the synthesized US-Gd_2O_3 nanoparticles synthesized via polyol free method with using citric acid in aqueous medium is given.

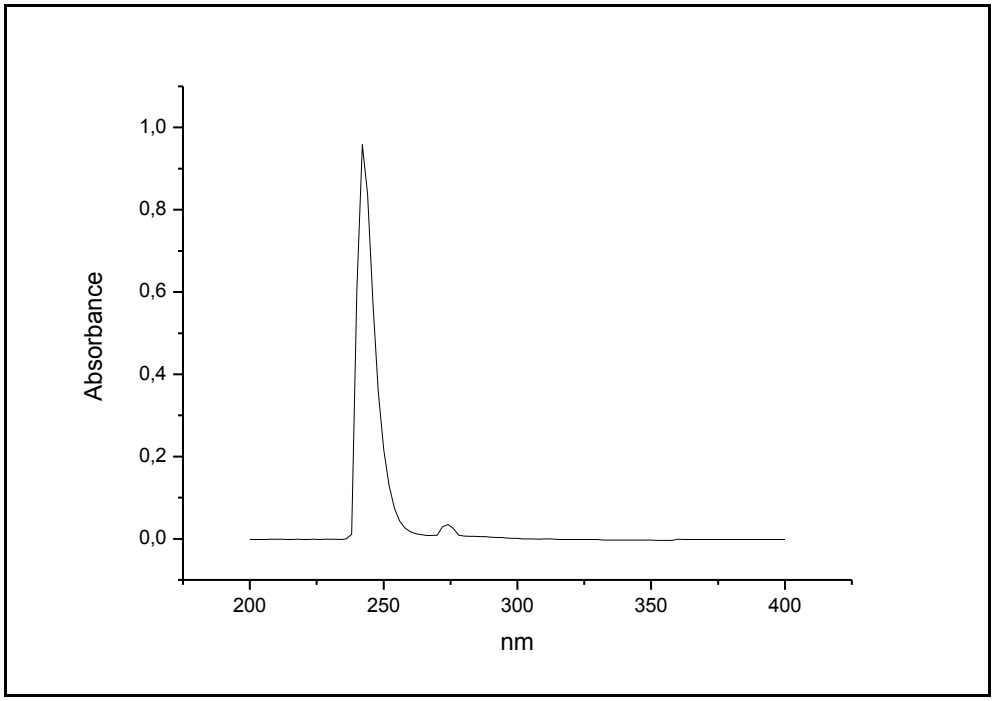

Figure 17 UV-VIS spectrum of the synthesized US-Gd_2O_3 nanoparticles synthesized via polyol free method with using citric acid in aqueous medium.

Nanoparticles were further characterized by CTEM. As mentioned above, the optimum molarity of citric acid was found as 0.6 M. However, high molarity of citric acid caused imaging problems during CTEM characterization. Large amount of citric acid was accumulated on TEM grid to prevent observation of US-Gd_2O_3 nanoparticles. Therefore, synthesized nanoparticles were washed with deionized water by using centrifugation two times. Then sample was diluted with deionized water for the characterization. For CTEM imaging, sample preparation was done by letting 1–2 drops of Gd_2O_3 in water dry on an

amorphous carbon coated 200 mesh grid. From the same sample, two different CTEM images were taken from different areas of CTEM grid.

In Figure 18 and Figure 19, CTEM image, and the size distribution graph of the synthesized US-Gd_2O_3 nanoparticles via polyol free method by using citric acid in aqueous medium are shown, respectively. This CTEM image was the first image that was taken from the sample. By looking at CTEM image, we can say that the synthesized nanoparticles are highly dispersed in aqueous medium. Their monodispersity is also supported by the size distribution graph. The size distribution graph was drawn by using ImageJ program with randomly selected 100 particles from CTEM image. According to this graph, it can be said that synthesized gadolinium oxide nanoparticles have narrow size distribution between 1-3 nm. The size distribution graph was drawn by randomly selecting 100 particles in CTEM image. According to size distribution graph, more than seventy-five percentages of synthesized US-Gd_2O_3 nanoparticles have narrow size distribution between 1-3 nm.

In Figure 18, CTEM image of the synthesized US-Gd_2O_3 nanoparticles via polyol free method by using citric acid in aqueous medium is given.

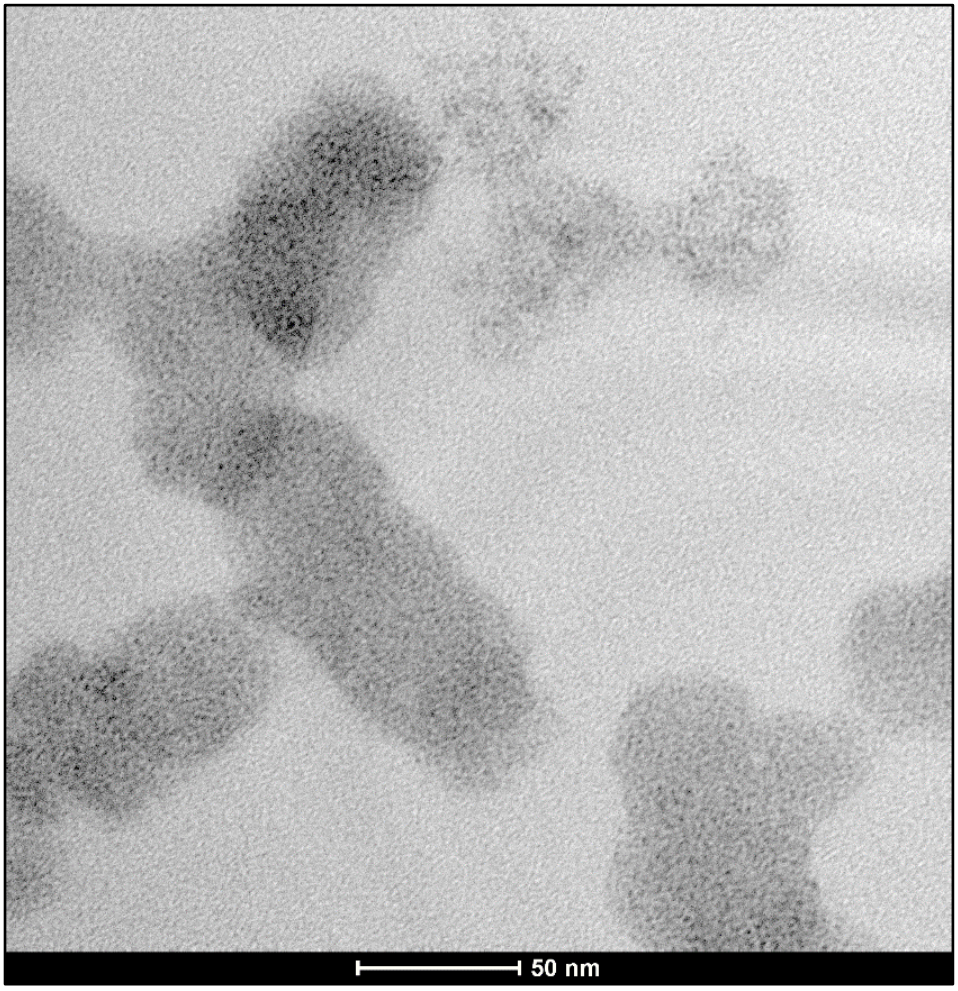

Figure 18 CTEM image of the synthesized US-Gd_2O_3 nanoparticles via polyol free method by using citric acid in aqueous medium.

In Figure 19, size distribution graph of the synthesized US-Gd_2O_3 nanoparticles via polyol free method by using citric acid in aqueous medium is given.

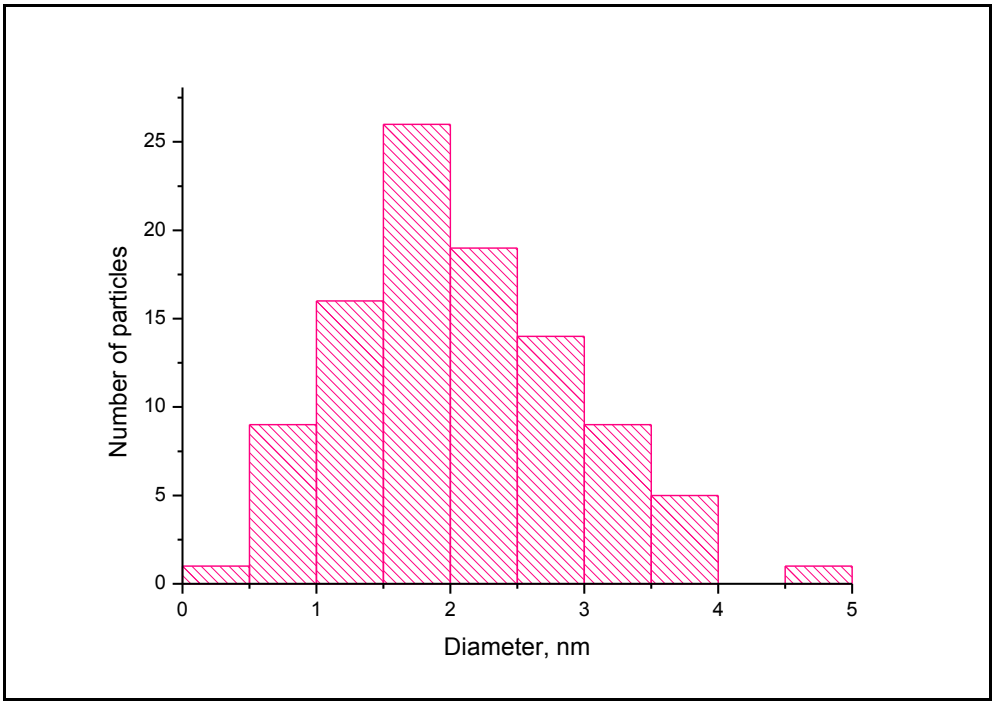

Figure 19 Size distribution graph of the synthesized US-Gd_2O_3 nanoparticles via polyol free method by using citric acid in aqueous medium.

CTEM image and size distribution graph of the synthesized US-Gd_2O_3 nanoparticles via polyol free method by using citric acid in aqueous medium are represented by Figure 20, and Figure 21, respectively. This CTEM image was the second image. CTEM image reveals that the synthesized nanoparticles are highly well dispersed in aqueous medium. The size distribution graph supports their monodispersity by giving details of their narrow size distribution that is between 1-3 nm. The size distribution graph was drawn by selecting random 100 particles in CTEM image by using ImageJ program. In this CTEM image, more than sixty-five percent of synthesized nanoparticles are found between 1-4 nm. This second image was taken to support the first image taken with more detail.

In Figure 20, CTEM image of the synthesized US-Gd_2O_3 nanoparticles via polyol free method by using citric acid in aqueous medium is given.

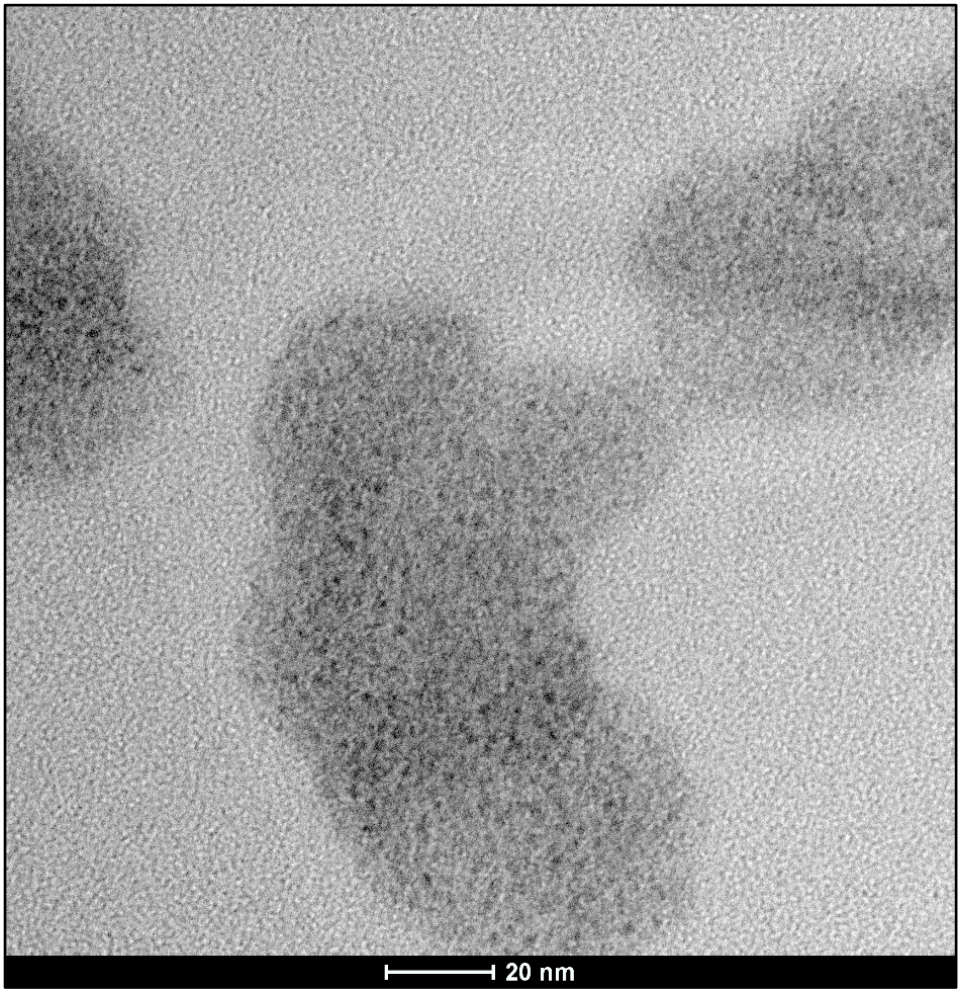

Figure 20 CTEM image of the synthesized US-Gd_2O_3 nanoparticles via polyol free method by using citric acid in aqueous medium.

In Figure 21, the size distribution graph of the synthesized US-Gd_2O_3 nanoparticles via polyol free method by using citric acid in aqueous medium is given.

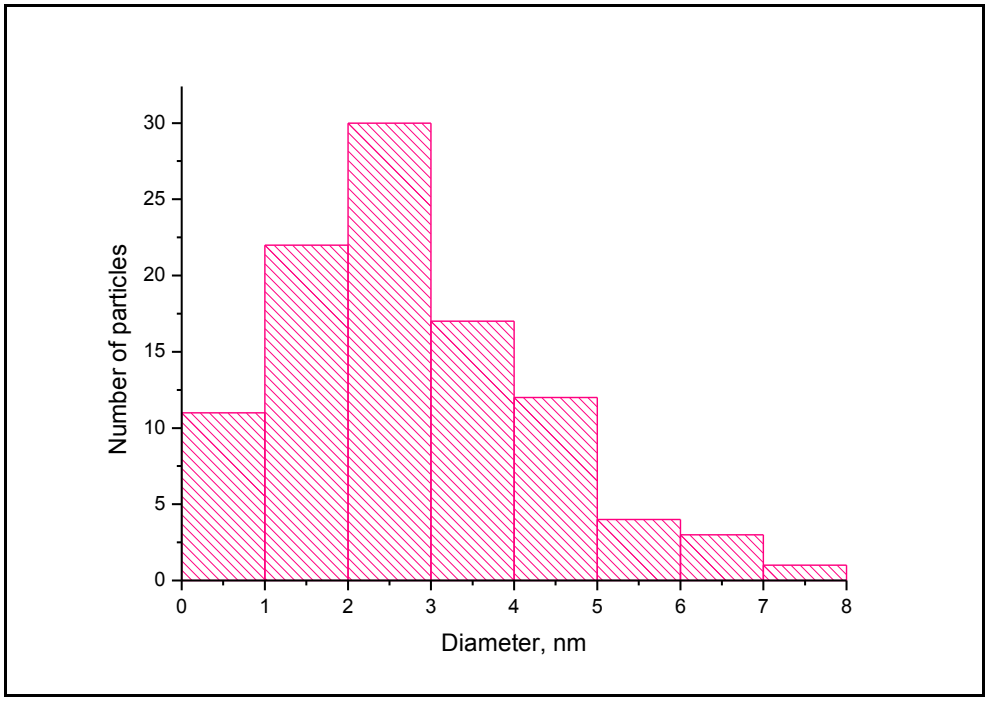

Figure 21 Size distribution graph of the synthesized US-Gd_2O_3 nanoparticles via polyol free method by using citric acid in aqueous medium.

CHAPTER 4

CONCLUSIONS

In the scope of this thesis, two different methods were used to synthesize US-Gd_2O_3 nanoparticles. The first method was polyol method since our aim was to synthesize nanoparticles in an ultra-small nano range. It is known that polyols control the particle size growth and they are used as stabilizer [56]. In this method, however, because of insufficient washing process which takes at least two months, the synthesized nanoparticles was not obtained as purely as desired to be used for characterization. Therefore any characterization results could not be obtained. That is why, at this stage, we have no results for polyol method to compare with other synthesis methods.

For the polyol free methods; three different synthesis methods were used. The first polyol free method was precipitation in basic medium. To characterize these nanoparticles XRD, SEM, EDX, CTEM techniques were used. EDX and XRD results show that gadolinium oxide nanoparticles were successfully synthesized. 100 nanoparticles were randomly selected from SEM image to measure their size distribution. According to the size distribution graph of randomly selected 100 nanoparticles in SEM image, size of the nanoparticles is found between 20-50 nm. XRD pattern also supports the nanosize of nanoparticles. The extensive broad peak around 29° in XRD pattern, which is the characteristic peak for the Gd_2O_3, provides us that our synthesized particles are in the range of nanometer. However, they are not ultra-small and according to CTEM image, agglomeration was observed in this method.

The second method for the synthesis of US-Gd_2O_3 nanoparticles was polyol-free method with citric acid in ethylene glycol medium. Citric acid was used as capping agent [40]. In this method, UV-VIS spectrometry and CTEM were used as characterization techniques. The peaks observed in UV-VIS spectrum show us that our synthesized nanoparticles are gadolinium oxide. From CTEM image, we can say that our nanoparticles are highly dispersed in ethylene glycol medium. The size distribution graph of 100 particles that were randomly selected from CTEM image was drawn by using ImageJ program. The size distribution graph also supports their monodispersity. According to this graph, more than fifty percent of synthesized gadolinium oxide nanoparticles have narrow size distribution between 2-4 nm which means they have been synthesized as ultra-small nanoparticles. It can be said that this polyol free method is desirable than the first method since UV-VIS spectrometry which is a feasible method to characterize nanoparticles is more applicable. Moreover, since the size of these US-Gd_2O_3 nanoparticles is between 2-4 nm, they were hardly characterized and image them by using CTEM. Therefore using UV-VIS spectrometry for characterization is advantageous for this method. These US-Gd_2O_3 nanoparticles were synthesized in ethylene glycol medium via this method; however, for the future application and usage of these ultra-small nanoparticles, having ethylene glycol medium is not highly desirable.

Since the synthesized US-Gd_2O_3 nanoparticles will be used in further biological applications, it has been tried to synthesize nanoparticles in aqueous medium. That is why; instead of ethylene glycol, deionized water was used for the synthesis of gadolinium oxide nanoparticles. This is the third method that was used to synthesize these US-Gd_2O_3 nanoparticles. CTEM and UV-VIS techniques were used for characterization particles synthesized in ultra-pure deionized water. According to the size distribution graph of randomly selected 100 nanoparticles from CTEM image, the synthesized nanoparticles are highly dispersed in aqueous medium and more than seventy-five percent of these nanoparticles have narrow size distribution between 1-3 nm. Also being highly

dispersed in the aqueous medium is highly desirable for their further biological application. UV-VIS results also prove that gadolinium oxide nanoparticles were successfully synthesized as ultra-small in aqueous medium. Moreover, 1.5-2.5 nm range is the optimum size range needed for maximal contrast enhancement in MRI [13]. When these results is compared to results that is obtained in the reference article [13], our synthesized US-Gd_2O_3 nanoparticles are more dispersed therefore can be more observable in CTEM images. We are also able to obtain UV-VIS spectrum of synthesized nanoparticles in aqueous medium which is not supplied in the reference article. These US-Gd_2O_3 nanoparticles are successfully synthesized in an ultra-small nanosize range (1-3 nm) and in aqueous medium. As a future work, with further purification, these US-Gd_2O_3 nanoparticles are going to be encapsulated in the apoferritin nanocage. They will be tested in bioactivity analysis to be used as contrast agent for MRI, and their longitudinal and transverse magnetic resonance relaxivities will be measured.

REFERENCES

[1] P. Borm, F. C. Klaessig, T. D. Landry, B. Moudgil, J. Pauluhn, K. Thomas, R. Trottier, and S. Wood, "Research Strategies for Safety Evaluation of Nanomaterials, Part V: Role of Dissolution in Biological Fate and Effects of Nanoscale Particles," *Toxicol. Sci.*, vol. 90, no. 1, pp. 23–32, 2006.

[2] G. A. Ozin, "Nanochemistry: Synthesis in diminishing dimensions," *Adv. Mater.*, vol. 4, no. 10, pp. 612–649, 1992.

[3] K. Khan, S. Rehman, H. U. Rahman, and Q. Khan, "Synthesis and Application of Magnetic Iron Nanoparticles," *Nanomagnetism*, 2014. [Online]. Available: http://www.onecentralpress.com/wp-content/uploads/2014/12/Chapter-6-Mg-08-Latest.pdf. [Accessed: 20-Jul-2017].

[4] Y. W. Jun, Y. M. Huh, J. S. Choi, J. H. Lee, H. T. Song, S. Kim, S. Yoon, K. S. Kim, J. S. Shin, J. S. Suh, and J. Cheon, "Nanoscale Size Effect of Magnetic Nanocrystals and Their Utilization for Cancer Diagnosis via Magnetic Resonance Imaging," *J. Am. Chem. Soc.*, vol. 127, no. 16, pp. 5732–5733, 2005.

[5] J. L. West and N. J. Halas, "Engineered Nanomaterials for Biophotonics Applications: Improving Sensing, Imaging, and Therapeutics," *Annu. Rev. Biomed. Eng.*, vol. 5, no. 1, pp. 285–292, 2003.

[6] J. Y. Park, M. J. Baek, E. S. Choi, S. Woo, J. H. Kim, T. J. Kim, J. C. Jung, K. S. Chae, Y. Chang, and G. H. Lee, "Paramagnetic ultrasmall gadolinium oxide nanoparticles as advanced T 1 MRI contrast agent: Account for large longitudinal relaxivity, optimal particle diameter, and in Vivo T1 MR images," *ACS Nano*, vol. 3, no. 11, pp. 3663–3669, 2009.

[7] H. B. Na, J. H. Lee, K. An, Y. I. Park, M. Park, I. S. Lee, D.-H. Nam, S. T. Kim, S.-H. Kim, S.-W. Kim, K.-H. Lim, K.-S. Kim, S.-O. Kim, and T. Hyeon, "Development of aT1 Contrast Agent for Magnetic Resonance Imaging Using MnO Nanoparticles," *Angew. Chemie*, vol. 119, no. 28, pp. 5493–5497, 2007.

[8] M. J. Sands and A. Levitin, "Basics of magnetic resonance imaging," *Semin. Vasc. Surg.*, vol. 17, no. 2, pp. 66–82, 2004.

[9] A. Klasson, "MRI Contrast Enhancement using Gd_2O_3 Nanoparticles," Linköping Studies in Health Sciences, PhD Thesis, 2008.

[10] T. Biswas, "Simulation Of Contrast Enhancement Of Various Brain Lesions (Without Iv Gadolinium) By Using The Neural," *Internet J. Radiol.*, vol. 14, no. 1, pp. 1–12, 2012.

[11] C. F. G. C. Geraldes and S. Laurent, "Classification and basic properties of contrast agents for magnetic resonance imaging," *Contrast Media Mol. Imaging*, vol. 4, no. 1, pp. 1–23, 2009.

[12] M.-A. Fortin, "Magnetic Nanoparticles Used as Contrast Agents in MRI: Relaxometric Characterisation," in *Magnetic Characterization Techniques for Nanomaterials*, Springer, Berlin, Heidelberg, 2017, pp. 511–555.

[13] A. T. M. Anishur Rahman, P. Majewski, and K. Vasilev, "Gd_2O_3 nanoparticles: size-dependent nuclear magnetic resonance," *Contrast Media Mol. Imaging*, vol. 8, no. 1, pp. 92–95, 2013.

[14] M. Ahrén, L. Selegård, F. Söderlind, M. Linares, J. Kauczor, P. Norman, P.-O. Käll, and K. Uvdal, "A simple polyol-free synthesis route to Gd_2O_3 nanoparticles for MRI applications: An experimental and theoretical study," *J. Nanoparticle Res.*, vol. 14, no. 8, 2012.

[15] M. Bottrill, L. Kwok, N. J. Long, M. Bottrill, E. Abel, T. Osborne, and N. Long, "Lanthanides in magnetic resonance imaging," *Chem. Soc. Rev.*, vol. 35, pp. 557–571, 2006.

[16] Z. Bakhtiary, A. A. Saei, M. J. Hajipour, M. Raoufi, O. Vermesh, and M. Mahmoudi, "Targeted superparamagnetic iron oxide nanoparticles for early detection of cancer: Possibilities and challenges," *Nanomedicine Nanotechnology, Biol. Med.*, vol. 12, no. 2, pp. 287–307, 2016.

[17] C. H. Cunningham, T. Arai, P. C. Yang, M. V. McConnell, J. M. Pauly, and S. M. Conolly, "Positive contrast magnetic resonance imaging of cells labeled with magnetic nanoparticles," *Magn. Reson. Med.*, vol. 53, no. 5, pp. 999–1005, 2005.

[18] L. Faucher, A.-A. Guay-Bégin, J. Lagueux, M.-F. Côté, É. Petitclerc, and M.-A. Fortin, "Ultra-small gadolinium oxide nanoparticles to image brain cancer cells in vivo with MRI," *Contrast Media Mol. Imaging*, vol. 6, pp. 209–218, 2011.

[19] "Gadolinium - Element information, properties and uses | Periodic Table." [Online]. Available: http://www.rsc.org/periodic-table/element/64/gadolinium. [Accessed: 07-Aug-2017].

[20] M.-F. Bellin, "MR contrast agents , the old and the new," *Eur. J. Radiol.*, vol. 60, pp. 314–323, 2006.

[21] A. J. L. Villaraza, A. Bumb, and M. W. Brechbiel, "Macromolecules , Dendrimers , and Nanomaterials in Magnetic Resonance Imaging : The Interplay between Size , Function and Pharmacokinetics," *Chem. Rev.*, vol. 110, no. 5, pp. 2921–2959, 2010.

[22] J.-M. Idée, M. Port, I. Raynal, M. Schaefer, S. Le Greneur, and C. Corot, “Clinical and biological consequences of transmetallation induced by contrast agents for magnetic resonance imaging : a review,” *Fundam. Clin. Pharmacol.*, vol. 20, pp. 563–576, 2006.

[23] T. Kanda, H. Oba, K. Toyoda, and K. Kitajima, “Brain gadolinium deposition after administration of gadolinium ‐ based contrast agents,” *Jpn. J. Radiol.*, vol. 34, no. 1, pp. 3–9, 2016.

[24] H.-J. Weinmann, R. C. Brasch, W.-R. Press, and G. E. Wesbey, “Characteristics of Gadolinium-DTPA Complex : A Potential NMR Contrast Agent,” *Am. Roentgen Ray Soc.*, pp. 619–624, 1984.

[25] “Contrast Media - Radiological Contrast Media Manufacturers.” [Online]. Available: http://www.regeimaging.in/product/contrast-media. [Accessed: 11-Aug-2017].

[26] S.-P. Lin and J. J. Brown, “MR Contrast Agents : Physical and Pharmacologic Basics,” *J. Magn. Reson. Imaging*, vol. 899, pp. 884–899, 2007.

[27] Z. Zhou and Z.-R. Lu, “Gadolinium-Based Contrast Agents for MR Cancer Imaging.” [Online]. Available: https://www.ncbi.nlm.nih.gov/pmc/articles/PMC3552562/#. [Accessed: 08-Aug-2017].

[28] M.-F. Bellin and A. J. Van Der Molen, “Extracellular gadolinium-based contrast media : An overview,” *Eur. J. Radiol.*, vol. 66, pp. 160–167, 2008.

[29] M. Rogosnitzky and S. Branch, “Gadolinium-based contrast agent toxicity : a review of known and proposed mechanisms,” *BioMetals*, 2016.

[30] J. Ramalho, M. Ramalho, M. Jay, L. M. Burke, and R. C. Semelka, “Gadolinium toxicity and treatment,” *Magn. Reson. Imaging*, vol. 34, no. 10, pp. 1394–1398, 2016.

[31] L. M. B. Burke, M. Ramalho, M. AlObaidy, E. Chang, M. Jay, and R. C. Semelka, "Self-Reported Gadolinium Toxicity: A Survey of Patients with Chronic Symptoms Lauren," *Magn. Reson. Imaging*, 2016.

[32] J. Fang, P. Chandrasekharan, X. Liu, Y. Yang, Y. Lv, C. Yang, and J. Ding, "Manipulating the surface coating of ultra-small Gd_2O_3 nanoparticles for improved T 1 -weighted MR imaging," *Biomaterials*, vol. 35, no. 5, pp. 1636–1642, 2014.

[33] J. Ramalho, R. Semelka, M. Ramalho, R. H. Nunes, M. AlObaidy, and M. Castillo, "Gadolinium-Based Contrast Agent Accumulation and Toxicity : An Update," *Am. J. Neuroradiol.*, pp. 1192–1198, 2016.

[34] H. Bin Na and T. Hyeon, "Nanostructured T1 MRI contrast agents," *J. Mater. Chem.*, vol. 19, no. 35, p. 6267, 2009.

[35] A. Klasson, M. Ahrén, E. Hellqvist, F. Söderlind, A. Rosén, P.-O. Käll, K. Uvdal, and M. Engström, "Positive MRI contrast enhancement in THP-1 cells with Gd_2O_3 nanoparticles," *Contrast Media Mol. Imaging*, vol. 3, pp. 106–111, 2008.

[36] T. Gayathri, N. M. Sundaram, and R. A. Kumar, "Gadolinium Oxide Nanoparticles for Magnetic Resonance Imaging and Cancer Theranostics," *J. Bionanoscience*, vol. 9, no. 6, pp. 409–423, 2015.

[37] J.-L. Bridot, a.-C. Faure, S. Laurent, C. Riviere, C. Billotey, B. Hiba, M. Janier, V. Josserand, J.-L. Coll, L. VanderElst, R. Muller, S. Roux, P. Perriat, and O. Tillement, "Hybrid Gd oxide nanoparticle multimodal contrast agents for in vivo imaging," *J. Am. Chem. Soc.*, vol. 129, no. 16, pp. 5076–5084, 2007.

[38] L. Faucher, Y. Gossuin, A. Hocq, and M.-A. Fortin, "Impact of agglomeration on the relaxometric properties of paramagnetic ultra-small gadolinium oxide nanoparticles," *Nanotechnology*, vol. 22, 2011.

[39] L. Faucher, M. Tremblay, J. Lagueux, Y. Gossuin, and M. A. Fortin, “Rapid synthesis of PEGylated ultrasmall gadolinium oxide nanoparticles for cell labeling and tracking with MRI,” *ACS Appl. Mater. Interfaces*, vol. 4, no. 9, pp. 4506–4515, 2012.

[40] A. T. M. Anishur Rahman, K. Vasilev, and P. Majewski, “Ultra small Gd_2O_3 nanoparticles: Absorption and emission properties,” *J. Colloid Interface Sci.*, vol. 354, no. 2, pp. 592–596, 2011.

[41] T. Skotland, T. Iversen, and K. Sandvig, “New metal-based nanoparticles for intravenous use : requirements for clinical success with focus on medical imaging,” *Nanomedicine Nanotechnology, Biol. Med.*, vol. 6, no. 6, pp. 730–737, 2010.

[42] S. A. Khan, S. Gambhir, and A. Ahmad, “Extracellular biosynthesis of gadolinium oxide (Gd_2O_3) nanoparticles, their biodistribution and bioconjugation with the chemically modified anticancer drug taxol,” *Beilstein J. Nanotechnol.*, vol. 5, no. 1, pp. 249–257, 2014.

[43] G. Singh, B. H. McDonagh, S. Hak, D. Peddis, S. Bandopadhyay, I. Sandvig, A. Sandvig, and W. R. Glomm, “Synthesis of gadolinium oxide nanodisks and gadolinium doped iron oxide nanoparticles for MR contrast agent,” *J. Mater. Chem. B*, 2016.

[44] S. Kumar, V. K. Meena, P. P. Hazari, and R. K. Sharma, “PEG coated and doxorubicin loaded multimodal Gadolinium oxide nanoparticles for simultaneous drug delivery and imaging applications.,” *Int. J. Pharm.*, 2017.

[45] K. Ni, Z. Zhao, Z. Zhang, Z. Zhou, L. Yang, L. Wang, H. Ai, and J. Gao, “Geometrical confined ultrasmall gadolinium oxide nanoparticles boost the T1 contrast ability,” *Nanoscale*, 2016.

[46] S. L. Mekuria, T. A. Debele, and H. Tsai, “Encapsulation of Gadolinium Oxide Nanoparticle (Gd_2O_3) Contrasting Agents in PAMAM Dendrimer Templates for Enhanced Magnetic Resonance Imaging in Vivo,” *ACS Appl. Mater. Interfaces*, vol. 9, pp. 6782–6795, 2017.

[47] F. C. Meldrum, B. R. Heywood, and S. Mann, “Magnetoferritin : In Vitro Synthesis of a Novel Magnetic Protein,” *Science*, vol. 257, pp. 522–523, 1992.

[48] P. M. Harrison and P. Arosio, “The ferritins: Molecular properties, iron storage function and cellular regulation,” *Biochim. Biophys. Acta - Bioenerg.*, vol. 1275, no. 3, pp. 161–203, 1996.

[49] P. Sánchez, E. Valero, N. Gálvez, J. M. Domínguez-Vera, M. Marinone, G. Poletti, M. Corti, and A. Lascialfari, “MRI relaxation properties of water-soluble apoferritin-encapsulated gadolinium oxide-hydroxide nanoparticles,” *R. Soc. Chem.*, pp. 800–804, 2009.

[50] N. D. Chasteen and P. M. Harrison, “Mineralization in Ferritin : An Efficient Means of Iron Storage,” *J. Struct. Biol.*, vol. 126, pp. 182–194, 1999.

[51] T. Douglas and V. T. Stark, “Nanophase Cobalt Oxyhydroxide Mineral Synthesized within the Protein Cage of Ferritin,” *Inorg. Chem.*, vol. 39, no. 8, pp. 1828–1830, 2000.

[52] L. Tian, C. Cao, and Y. Pan, “The influence of reaction temperature on biomineralization of ferrihydrite cores in human H-ferritin,” *Biometals*, vol. 25, pp. 193–202, 2012.

[53] R. Tsukamoto, K. Iwahori, M. Muraoka, and I. Y. Ã, “Synthesis of Co3O4 Nanoparticles Using the Cage-Shaped Protein , Apoferritin,” *Bull. Chem. Soc. Jpn.*, vol. 78, no. 11, pp. 2075–2081, 2005.

[54] M. Yamaki, “Single Molecular Functional Assay of Ferritin Arrays,” *Adv. Biophys.*, vol. 34, pp. 191–203, 1997.

[55] “ImageJ.” [Online]. Available: http://imagej.net/ImageJ. [Accessed: 10-Sep-2017].

[56] S. Laurent, D. Forge, M. Port, A. Roch, C. Robic, L. Vander Elst, and R. N. Muller, “Magnetic iron oxide nanoparticles: Synthesis, stabilization, vectorization, physicochemical characterizations and biological applications,” *Chem. Rev.*, vol. 108, no. 6, pp. 2064–2110, 2008.